COMPACT MICROSTRIP BANDPASS FILTER BASED ON CONCENTRIC RING RESONATORS

A THESIS SUBMITTED TO

THE GRADUATE SCHOOL OF NATURAL AND APPLIED

SCIENCES OF

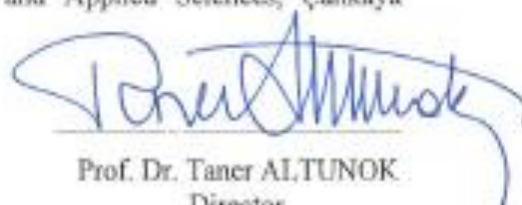ÇANKAYA UNIVERSITY

BY

MOHAMMED ABDULRAZZAQ AZEEZ AL-MIHRAB

IN PARTIAL FULFILMENT OF THE REQUIREMENTS THE DEGREE OF

MASTER

IN

THE DEPARTMENT OF

ELECTRONIC AND COMMUNICATION ENGINEERING

JUNE2014

Title of the Thesis: **Compact Microstrip Bandpass Filter Based on Concentric Ring Resonators.**

Submitted by **Mohammed Abdulrazzaq Azeez AL-MIHRAB**

Approval of the Graduate School of Natural and Applied Sciences, Çankaya University.

Prof. Dr. Taner ALTUNOK
Director

I certify that this thesis satisfies all the requirements as a thesis for the degree of Master of Science.

Prof. Dr. Celal Zaim ÇIL
Head of Department

This is to certify that we have read this thesis and that in our opinion it is fully adequate, in scope and quality, as a thesis for the degree of Master of Science.

Prof. Dr. Yusuf Ziya UMUL
Supervisor

Examination Date: 10.06.2014

Examining Committee Members

Prof. Dr. Yusuf Ziya UMUL	(Çankaya Univ.)	
Assist. Prof. Nursel AKÇAM	(Gazi Univ.)	
Dr. H. Deniz BAŞDEMİR	(Çankaya Univ.)	

STATEMENT OF NON-PLAGIARISM PAGE

I hereby declare that all information in this document has been obtained and presented in accordance with academic rules and ethical conduct. I also declare that, as required by these rules and conduct, I have fully cited and referenced all material and results that are not original to this work.

Name, Last Name : Mohammed Abdulrazzaq Azeez AL-MIHRAB

Signature :

Date : 10.06.2014

ABSTRACT

COMPACT MICROSTRIP BANDPASS FILTER BASED ON CONCENTRIC RING RESONATORS

AL-MIHRAB, Mohammed Abdulrazzaq Azeez

M.Sc., Department of Electronic and Communication Engineering

Supervisor:Prof. Dr. Yusuf Ziya UMUL

June 2014, 62 Pages

In this dissertation, a new dual mode microstrip bandpass filter has been presented for the requirements of modern wireless communication systems. The filter has been constructed from double concentrated square loop resonators; each resonator is based on applying step impedance resonator generator on each side of closed resonator. The proposed bandpass filters have been designed using a substrate with a dielectric constant of 10.8 and thickness of 1.27mm at 2.43GHz and 5.75 GHz resonant frequencies. These filters have compact size and narrow band response which are the requirements of mobile wireless communication systems. The performance of suggested filters have been analyzed using Microwave office software package and Sonnet simulator, which are widely adopted in microwave research and industry. The output results showed that this filter possesses very good frequency responses and high selectivity as well as blocked 2nd harmonic in out of band regions.

Keywords: Microstrip Bandpass Filter, Narrow Bandpass Filter, Compact Filters, Double Ring Concentric Resonators, Step Impedance Resonator (SIR).

ÖZ

HALKA REZONATÖRLER İLE OLUŞTURLMUŞ MİKROŞERİT BANT GEÇİREN FİLTRE TASARIMI

AL-MIHRAB, Mohammed Abdulrazzaq Azeez

Yüksek Lisans, Elektronik ve Haberleşme Mühendisliği Anabilim Dalı

Tez Yöneticisi:Prof. Dr. Yusuf Ziya UMUL

Haziran 2014,62 Sayfa

Bu tezde yeni bir çift mod mikroşeritli geçiş filtresi, modern kablosuz iletişim sistemlerinin gereksinimleri için sunulmuştur.Filtre çift konsantre kare döngü rezonatörlerden meydana gelmiştir. Her rezonatör kapalı bir rezonatörün her iki tarafında adım empedans resonator-jeneratörü uygulanmasınadayanır.Önerilen bu bant-geçirgen filtreler 2.43 ve 5.75 GHz frekanslarında,dielektrik sabiti 10.8 vekalınlığı 1.27mm olan alt tabaka kullanılarak tasarlanmıştır. Bu filtreler mobil kablosuz iletişim sistemlerinin gereksinimlerinı karşılamak üzere küçükboyutlu ve dar-bant tepki verecek şekildedir. Önerilen bu filtrelerin performans analizleri, mikrodalga ofis yazılım paketi ve Sonnet programları ile incelenmiştir. Bu programlar mikrodalga araştırmave endüstrisinde yaygın olarak kullanılmaktadır. Sonuçlar bu filtrenin, çok iyi bir frekans yanıtı ve yüksek seçiciliğe sahip olduğunu göstermektedir. Ayrıca bant bölümlerinin dışında 2 harmonik bastırılmıştır.

AnahtarKelimeler: Mikroşerit Bant Geçirgen Filtre, Dar Bant Geçirgen Filtre, Kompakt Filtreler, Çift Halkalı Eş Resonatörler, Adım Empedans Rezonatörü(AER).

ACKNOWLEDGEMENTS

TABLE OF CONTENTS

CHAPTERS:

LIST OF TABLES

TABLES

LIST OF FIGURES

FIGURES

FIGURES

FIGURES

LIST OF ABBREVIATIONS

AC   Alternating Current

BPF   Bandpass Filter

DC   Direct Current

DSR   Dual Spiral Resonator

EMI   Electromagnetic Interference

EM   Electromagnetic

HTS   High Temperature Superconducting

IL   Insertion Loss

ILM   Insertion Loss Method

IPM   Image-Parameter Method

LAN   Local Area Network

LPP   Lowpass Prototype

PCB   Printed Circuit Board

RF   Radio Frequency

RT/Duroid   Rogers Duroid

SIR   Stepped Impedance Resonator

TE   Transverse Electric

TEM   Transverse Electromagnetic

TM   Transverse Magnetic

VSWR   Voltage Standing Wave Ratio

LIST OF SYMBOLS

α	Attenuation Coefficient
β	Phase Constant
R	Resistance
L	Inductance
C	Capacitance
λ	Wavelength
λ_g	Guided-Wavelength
$\lambda_\circ$	Free Space Wavelength
λ_{g0}	Guided Wavelength at Resonant Frequency
Ω	Ohm
V	Voltage
I	Current
μ_r	Relative Permeability
ε_r	Relative Permittivity
$\mu_\circ$	Free Space Permeability
$\varepsilon_\circ$	Free Space Permittivity
f_o	Resonant Frequency
ω	Angular Frequency
f	Frequency
ω_o	Centre Frequency of Bandpass Filter
βl	Electrical Length
v_p	Phase Velocity
$Z_\circ$	Characteristic Impedance
I/O	Input and Output
$J_n(kr)$	Bessel Function of 1st Kind of Order n
$N_n(kr)$	Bessel Function of 2nd Kind of Order n

T	Thickness of Conductor
h	High of Dielectric Between Conductor and Substrate
Γ	Reflection Coefficient
C_d	Capacitance of Transmission Line with Dielectric Filing
c	Free Space Velocity of Light ($\approx 3 \times 10^8 m/s$)
Δ	3 *dB* Fractional Bandwidthof Bandpass Filter
ε_{eff}	Effective Dielectric Constant
S_{ij}	Transmission Coefficient
S_{ii}	Reflection Coefficient

CHAPTER 1

INTRODUCTION

1.1. Background

In present wireless communication scenario, the development of new network signal processing algorithms and innovative hardware devices is fundamental to support the rapidly growing expansion of new and sophisticated services. In particular, modern microwave architectures have to satisfy more and more stringent requirements concerning their performances, together with a general criterion of compactness and easy integration with other systems. In the field of the microwave pass-band filters, which play a fundamental role in many applications [1]. Communication system is simply the transferred data information from sender to receiver. Microstrip filter can be any component which is used on the transmitter and receiver of microwave communication system. It is situated at the place of ending transmitter and also in the beginning of receiver. The microstrip filter transmission at transmitter and receiver are the transmission medium [2]. The resonators may be classified into planar resonators and non-planar resonators. The planar resonators are commonly achieved by using the microstrip technology. Microstrip line resonators are related to highly planar resonators. The microstrip resonator line has many benefits to decrease the resonator size. One ofmost adopted methods to miniaturize the microstrip line resonator is meandering the microstrip resonator. The open loop meandered microstrip line resonator is less than $\lambda_{g0}/8$ by $\lambda_{g0}/8$, where λ_{g0} is the guided wavelength at resonant frequency [3]. For more resonator miniaturization using meandering the microstrip line, the microstrip line must have too narrow line. However, generally, this will reduce the quality factor of the resonator as the line becomes narrower. This problem can be solved by using High Temperature Superconducting (HTS) materials but the cooling requirements eliminate the miniaturization advantage. On the other hand, non-planar resonators possess relatively bigger quality factor as compared to planar resonators. These non-planar resonators are bulky, however, they are used by the wireless systems where the

electrical responses are more vital and necessary than filter size. For instance, the waveguide cavity filters have been used in many applications of cellular base stations and satellite transponders [4]. The proposed microstrip bandpass filters in this dissertation have been constructed from double concentrated square loop resonators, each resonator is based on applying step impedance resonator generator on each side of closed square loop resonator. These filters have compact sizes and narrow band responses which are the requirements of mobile wireless communication systems.

1.2. The Literature Survey

In 1995,J. S. Hong, and M. J. Lancaster [5], developed a type of dual-mode high selectivity and narrowband microstrip BPFsconstructed from a meander loop resonator for compactness purposes. This filter was designed at center frequency of 1.58 GHz and a 2.5% bandwidth. Themicrostrip filter was designed on a RT/Duriod substrate with dielectric constant of 10.8 and a thickness of 1.27 mm .

In 2000,J. S. Hong, and M. J. Lancaster [6], displayed a design of narrow band microstrip bandpass filters that are based on open-loop resonators. These filters offer a single pair of attenuation poles at finite frequencies. By the way, two examples of this design consist of a sixth order filter with a fractional bandwidth of 7.331% at 955 MHz and an eight-pole filter with a fractional bandwidth of 10.359% at 985 MHz has been described. The filter is modeled on an RT/Duroid substrate with a relative dielectric constant of 10.8 and a thickness of 1.27 mm.

In 2001,M. Matsuo, H. Yabuki, and M. Makimoto [7], concentrated on a ring resonator having an impedance step as perturbation form. Full analysis method about resonance characteristics and generation of attenuation poles obtained by this resonator structure has been presented and explained. RT/Duroid has been selected for the dielectric substrate, having a relative dielectric constant of 10.5, thickness of 1.27 mm, as well as loss tangent of 0.002.

In 2002, A. Görür [8], proposed a style of dual-mode microstrip square loop filter which is based on the microstrip slow-wave open-loop resonator. The that the designed dual-mode microstrip filter has a wide stopband including 1st spurious resonance frequency. Besides, it has a miniaturization percentage of about 50% at the resonant frequency, as compared to dual-mode microstrip patch, cross-slotted patch,

ring resonator and square loop bandpass filters. The bandpass filter was modeled on an RT/Duroid substrate possessing a thickness of 1.27 mm and a relative dielectric constant of 10.2 .

In 2003, A. Görür, Ceyhun Karpuz, and Mustafa Akpinar [9], used degenerate modes of a dual-mode microstrip square loop resonator to develop dual-mode microstrip bandpass filter with capacitively loaded open-loop arms. This bandpass filter has been designed at the center frequency of 1.603 GHz and a 0.75% bandwidth to verify the design of compact microstrip filters. The proposed filter has a miniaturization percentage of about 59% at the resonant frequency, as compared to dual-mode microstrip patch, cross-slotted patch, ring resonator and square loop bandpass filters. The bandpass filter was modeled on an RT/Duroid substrate having a thickness of 1.27 mm and a relative dielectric constant of 10.2 .

In 2005, C.Lugo and J. Papapolymerou [10], suggested dual-mode microstrip triangular loop resonator bandpass filter (BPF) design. The filter has frequency responses with single real finite frequency transmission zero and single imaginary finite frequency zero on each side of the passband. Based on the perturbation effect, the strength of the coupling among degenerate modes makes the zeros to replace their axis locations from real to imaginary and vice versa while keeping their magnitude. This phenomenon produces frequency responses that are possible for uses with irregular requirements. The filter has insertion loss ranging from 0.82 dB to 1.4 dB with 8% bandwidth at 10 GHz. Also, they have compact size and easy in fabrication. The adopted substrate in this design is related to Rogers Duroid, with substrate thickness of 25 mils and a dielectric constant of 10.2 .

In 2007,Y. X. Wang, B. Z. Wang, and J. Wang [11], presented new dual-mode microstrip BPF with wide stop-band.This filter uses square loop resonator with tree shaped patches placed to all four internal corners of the loop. The splitting mode is realized by making a small cut at a $45°$ offset from its dual orthogonal modes. This microstrip BPF has a wide stop-band especially in the first spurious resonance frequency. The center frequency can be tuned. Moreover, the designed filter has a more compactness as compared with conventional dual mode bandpass filters at the similar central frequency. The used RT/Duroid substrate in this filter has a relative

dielectric constant of 10.8 and a thickness of 1.27mm fundamental frequency of 1.59 GHz.

In 2009, S.K.Hashemi and D. M.Syahkal [12], proposeda class of miniaturized microwave BPF. These filters consist of multilayer ring resonators (MRR) technique which is suitable to narrow band and ultra-wideband (UWB) BPFs. This generation of filters has small circuit size and easy in fabrication. Many attenuation poles are found and can be easily shift to the left or right of the passband. The overall dimensions of the filters are to be around 2 mm × 2 mm × 1 mm. Three substrates with height of$h_1 = h_2 = h_3 = 0.381$mm and relative dielectric constant of$\varepsilon_{r1} = \varepsilon_{r2} = \varepsilon_{r3} = 9.8$ have been used.

In 2010, M. Zhou, etal. [13], proposed compact dual mode microstrip bandpass filter based on resonator-embedded structure. Dual transmission zeros are placed to enhance the selectivity of the filter. In addition, source-load capacitive coupling is submitted to form a transmission zero above the passband. The filter is designed on 2.28 GHz with 300 MHz bandwidth. The filter size is smaller than $0.21\lambda \times 0.25\lambda$, where λ is guided wavelength at the central frequency. The used substrate in this design hasa thickness of 0.635 mm and a relative dielectric constant of 9.5.

In 2011, R. Phromloungsri, etal. [14], presented bandpass filter design based on proposed stepped-impedance resonator (SIR) technique. This resonator is made up of a quarter wavelength coupler with SIR principle attached at the end of the lines desined at 0.9 GHz. Each port has a step impedance feed line to set the impedance of filter closed to the value of characteristic impedance Z_0. This resonator can eliminate the spurious response at $2f_0$ and $3f_0$. This filter can block the 2nd and 3rd in out of band region. The resonator is designed on the substrate of RF60 with ε_r =6.0 ,h=1.52 mm.

In 2014, D. Bukuru, etal. [15], developed a miniaturized microstrip bandpass filter based on a rectangular dual spiral resonator (DSR). The rectangular DSR bandpass filter is centered at 3.65 GHz to suit for Wireless LAN (IEEE802.11y) application. The proposed filter offers transmission zero at the high side of out-of-band response. The total circuit area of the miniaturized bandpass filter is$0.145\lambda_g$ by $0.135\lambda_g$,at 3.65

GHz. For demonstration purposes, a compact DSR bandpass filter is designed on the Taconic RF-35 (tm) substrate(ε_r= 3.5, h = 0.508 mm, and loss tangent = 0.0018) .

1.3. The Main Goals of This Thesis

The plan of this dissertation is to present compact microstrip bandpass filter design structure suitable for use in modern wireless mobile applications. The proposed filter design is based on double concentrated stepped impedance square loop resonators which have been modeled, simulated and evaluated using EM simulator Microwave Office 2009.

1.4. Thesis Layout

This thesis is organized as follows:

- Chapter two includes the fundamental principles of microstrip bandpass filters and their applications.
- Chapter three provides the fundamental basics of the dual-mode square ring resonators.
- Chapter four contains design and a results of simulation of proposed model of microstrip filter.
- Chapter five includes the conclusions and the recommendations for future work.

CHAPTER 2

THEORITICAL FUNDAMENTALS OF MICROSTRIP

2.1. Introduction

This chapter shows an overview of the theoretical background of microwave engineering used in this dissertation. The chapter starts with the basic definitions followed by a discussion of the propagations modes that exists in microstrip technology as well as discontinuities and stub tunes that may occur. Scattering matrix is also introduced as well as ABCD parameters, Richard's transformation, Kurodas's Identities and some construction methodologies. Also, this chapter describes theoretically the design procedure and basics of lowpass and the bandpass filters .

2.2. Microwave

Microwave means alternate current signals with a range of frequencies between 300 MHz and 300 GHz, corresponding to a wavelength (λ) between $\lambda = c/f = 1m$ (300 MHz) and $\lambda = 1mm$ (300 GHz). Most of the present research and wireless communications cover this frequencies range. When using these frequencies there are several aspects that have to be taken into account, i.e. radiation, coupling electromagnetic issues and frequency response of lumped (discrete entities that estimate the performance of the distributed system under assured assumptions) circuit elements [16].Standard circuit theory cannot solve the usual microwave problems for high frequencies (short wavelengths). Most of the times microwave components are distributed elements were phase and current change significantly with the physical dimensions of the device due to a dependence related to the microwave length. Thus, at low frequencies the wavelength is larger and there are not significant changes in the phase values across the component. In high frequencies the wavelengths are much shorter than the dimensions of the component [17].

2.3. Transmission Lines

Transmission lines are a very important factor in the design of integrated/high frequency circuits. Their length is expressed as a multiple or sub multiple of an electric or electromagnetic propagating signal wavelength and it can be expressed by degrees or radians.

Circuit theory and transmission line theory essentially differ in the electrical size. Circuit analysis assumes the physical dimension of a network much less than electrical wavelength. On the other hand, a transmission line may be a significant part of one or quite a lot of wavelengths.

Important factors that describe a RF/microwave design are cost, electric performance, power and reliability. Costs may be reduced by using a cheap technology, a cheap substrate, a set of uncomplicated elements and a minimum number of interconnection. Every printed transmission lines have their conductors impressed in a relatively small substrate. These lines can be uniform or non uniform, homogeneous or non homogeneous, lossy or lossless, protected or non protected, monolayer or multilayer and can be based in one or several substrates, i.e. different dielectrics. In uniform lines the characteristic impedance does not vary throw the line (opposite in the non uniform lines). In practice we can vary this impedance by varying the strip width.

When transmission lines have different dielectric such as microstrip lines, the transmission velocity depends on the transversal geometry of the line and the dielectric constants of the different mediums such as air and substrate material. Considering the dielectric constant of the line higher than the dielectric constant of the air and lower then the substrate material then the propagation of the electromagnetic waves is not realized as in a TEM (Transverse Electromagnetic) environment.

In a low loss transmission line the conductor thickness is 3 to 5 times higher than the human skin. Lossy transmission lines (conductor thickness smaller than the layer composition) can be used in the construction of terminals and attenuators.

When combining different transmission lines it is useful to use multiple layers. With multiple layers it is possible to combine radio-frequencies and digital functions in an

single module, i.e. the final circuit will be smaller, light, more reliable and will have more performance and lower costs [18].

Unshielded transmission lines are in direct contact with the air so they have to be protected from external radiation and Electromagnetic Interference (EMI) as Figure 1 illustrates.
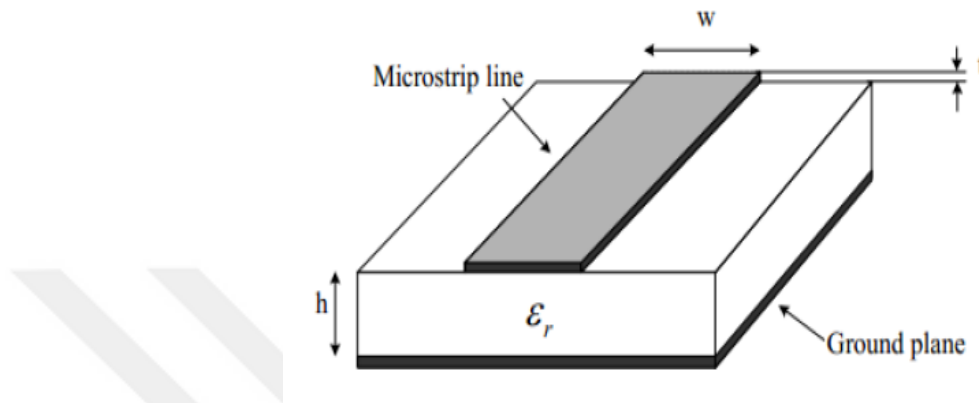
Figure 1: Unshielded transmission line

This protection is provided by a shield around the transmission line [19].

2.3.1. Propagation

TEM (Transverse Electromagnetic Waves) is the Stripline propagation mode. The conductor path is surrounded by similar dielectric materials, i.e. there are none electric or magnetic fields in the propagation direction. Thus, it possesses a phase velocity equivalent to light velocity. One other common example beside Stripline that supports TEM propagation is the coaxial medium.

Microstrip lines propagation is characterized by a combination of TM (Transverse Magnetic) and TE (Transverse Electric). TM means that magnetic fields in the propagation direction do not exist, and TE means that there are not any electric fields in the propagation direction. Notice that the dielectric of the upper part of the microstrip line is air and the bottom is a PCB (Printed Circuit Board). In this case the TEM is not supported because the waves phase velocity of the air is different from the velocity in the PCB. However, in a lower frequency (<=66 GHz) the magnetic and electric fields are sufficiently small in a way that these two propagation modes

join themselves (quasi-TEM). With low frequencies most of the electromagnetic field is distributed through the air, and with high frequencies the electromagnetic field travels in the PCB dielectric direction [18].

Therefore, a transmission line filled with a uniform dielectric can support a single and well-defined mode of propagation over a specified range of frequencies. This happens in TEM for coaxial lines, TE for waveguides, etc.

2.3.2. Microstrip Transmission Lines

A microstrip transmission line consists on a dielectric material sandwiched between metalized conductor(s) with a specific metallization circuit conductor on top and ground-plane on the back, as illustrated in Figure 2 .
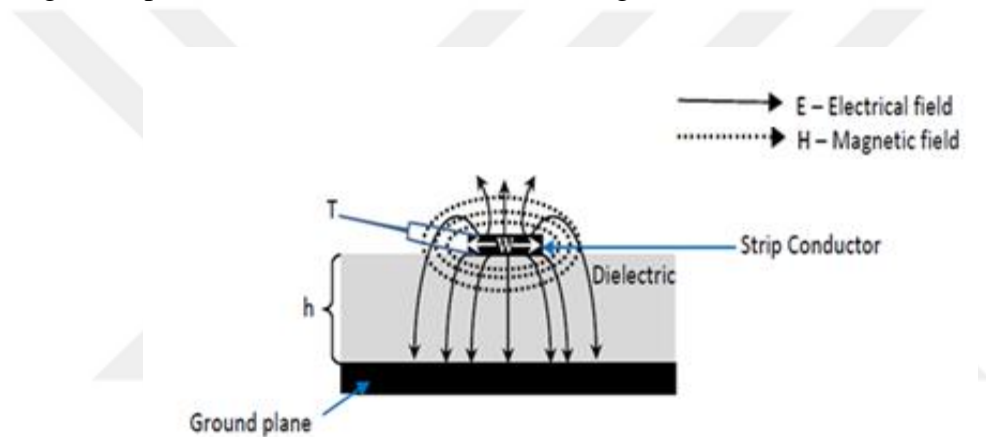
Figure 2: Microstrip line details

This technology that can be easily integrated with other passive and microwave devices. The conductor with a specific Thickness (T) is printed on a thin grounded dielectric substrate with a specific height (h) and relative permittivity (ε_r).

Microstrip transmission lines characteristics include:
- Good geometry that provides power handling, moderate radiation loss and reasonable dispersion over a wide characteristic impedance range (about15 to 150 Ohms) [21].
- Easy incorporations of active devices, diodes and transistors.
- Transmission of DC and AC signals.
- Line wavelength is considerably reduced from its free-space value due to the substrate fields.

- The structure can support moderately high voltages and power levels [20].

Concerning the design issues there are a few variables of high importance such as characteristic impedance and the propagation coefficient. Therefore, a microstrip transmission line is a distributed parameter network. where voltages and currents can vary in magnitude and phase along the line length. The voltage (V) and current (I) on a transmission line along the z axis are given by:

$$V(z) = V_\circ^+ e^{-\gamma z} + V_\circ^- e^{+\gamma z} \tag{2.1}$$

$$I(z) = I_\circ^+ e^{-\gamma z} + I_\circ^- e^{+\gamma z} \tag{2.2}$$

The $e^{-\gamma z}$ term describes wave propagation in the $+z$ direction and the $e^{+\gamma z}$ term represents the propagation in the $-z$. The complex propagation constant γ is given by:

$$\gamma = \alpha + j\beta = \sqrt{(R + j\omega L)(G + j\omega C)} \tag{2.3}$$

Where α represents the attenuation coefficient given by $neper.m^{-1}$, the phase coefficient β give by $radians.m^{-1}$, R and L are the series resistance and inductance per unit length and G and C are the shunt conductance and capacitance per unit length. The real part α causes signal amplitude to decrease along the transmission line and the imaginary part or phase constant β determines the sinusoidal amplitude/phase of the signal along the transmission line at a constant time [22]. These terms are not constants because they depend on the material, frequency or geometry in use.

Another important issue is the characteristic impedance. If we consider a travelling wave in the transmission line regardless its path (forward or backwards), the ratio of voltage to current is the characteristic impedance. Meaning that the impedance can be defined as:

$$Z_\circ = \frac{R + j\omega L}{\gamma} = \sqrt{\frac{R + j\omega L}{G + j\omega C}} \, \Omega \tag{2.4}$$

Assuming a lossless line with perfect conductors and dielectric material i.e. if no conducting currents exists between the two conductors and for that matter G=0 and R=0, then the propagation coefficient is:

$$\gamma = \alpha + j\beta = j\omega\sqrt{LC} \qquad (2.5)$$

Where at sufficiently high ratio frequencies the phase constant is given by Eq.(2.6).

$$\beta = \omega\sqrt{LC} \qquad (2.6)$$

For a lossless transmission line (attenuation constant $= 0$), the characteristic impedance can be written as:

$$Z_\circ = \sqrt{\frac{L}{C}}\ \Omega \qquad (2.7)$$

A wider microstrip line occupies more area in the dielectric which results in larger capacitance per length. Considering C_d the capacitance of the transmission line with dielectric filing and C_{free} the capacitance that has no dielectric filing we have the following relation:

$$C_d = \varepsilon_r C_{free} \qquad (2.8)$$

However, the inductance per unit length is independent of the line's dielectric and is given by:

$$L = \frac{1}{c^2 C_{free}} \qquad (2.9)$$

In the above equation c is the propagation velocity of the electromagnetic wave in free space ($\approx 3 \times 10^8 m/s$).

Eq. (2.9) can be used in Eq. (2.7) to obtain Eq. (2.10).

$$Z_\circ = \sqrt{\frac{L}{C}} = \frac{1}{c\sqrt{\varepsilon_r}C_{free}} \qquad (2.10)$$

The phase velocity for a TEM wave can be written as:

$$v_p = \frac{c}{\sqrt{\varepsilon_r}}$$

(2.11)

The wavelength of such propagation type is defined as:

$$\lambda = \frac{\lambda_\circ}{\sqrt{\varepsilon_r}}$$

(2.12)

Where $\lambda_\circ$ is the free space wavelength. Therefore the wavelength is proportioned to the square root of the relative permittivity of the uniform dielectric material in which the line is implemented. So, for large permittivity materials the distributed components became shorter resulting in less occupied space [23].

Still, a microstrip line cannot support a pure TEM wave (phase velocity varies from the dielectric region ($v_p = c/\sqrt{\varepsilon_r}$) to the air region ($v_p = c$), so the exact fields in a microstrip environment (quasi-TEM propagation mode) constitute a hybrid TM-TE wave, and for these matter approximations for the phase velocity, propagation constant and characteristic impedances will be obtained by the following quasi-static solutions[24]:

$$v_p = \frac{c}{\sqrt{\varepsilon_{eff}}}$$

(2.13)

$$\beta = k_\circ \sqrt{\varepsilon_{eff}}$$

(2.14)

$$k_\circ = w\sqrt{\mu_\circ \varepsilon_\circ}$$

(2.15)

In the above equations v_p is the phase velocity and β is the propagation constant. Phase velocity also depends on the effective dielectric constant (ε_{eff}) of the microstrip line which has a value between the air dielectric (1) and the region dielectric(ε_r). It also depends on the conductor width (w) and the substrate thickness (h) as follows [17]:

$$\varepsilon_{eff} = \frac{\varepsilon_r + 1}{2} + \frac{\varepsilon_r - 1}{2} \times \frac{1}{\sqrt{1 + 12 \times \frac{h}{w}}}$$

(2.16)

Once the dielectric constant is known the characteristic impedance of the line can be calculated by Eq. (2.17).

$$Z_\circ = \begin{cases} \dfrac{60}{\sqrt{\varepsilon_{eff}}} \ln\left(\dfrac{8h}{w} + \dfrac{w}{4h}\right) & for \ \dfrac{w}{h} \le 1 \\[3ex] \dfrac{120\pi}{\sqrt{\varepsilon_{eff}}\left(\dfrac{w}{h} + 1.393 + 0.667 \ln\left(\dfrac{w}{h} + 1.444\right)\right)} & for \ \dfrac{w}{h} \ge 1 \end{cases} \tag{2.17}$$

Let ψ represents the ratio $\dfrac{w}{h}$ and $\mathcal{B}$ refers to $B - 1$ based on specific characteristic impedance and dielectric constant takes the following form Ref. [17]:

$$\psi = \begin{cases} \dfrac{8e^A}{e^{2A} - 2} \ for \psi < 2 \\[3ex] \dfrac{2}{\pi}\left[\mathcal{B} - \ln(2B - 1) + \dfrac{\varepsilon_r - 1}{2\varepsilon_r}\left(\ln(\mathcal{B}) + 0.39 - \dfrac{0.61}{\varepsilon_r}\right)\right] for \psi > 2 \end{cases} \tag{2.18}$$

$$A = \frac{Z_\circ}{60}\sqrt{\frac{\varepsilon_r + 1}{2}} + \frac{\varepsilon_r - 1}{\varepsilon_r + 1}\left(0.23 + \frac{0.11}{\varepsilon_r}\right) \tag{2.19}$$

$$B = \frac{377\pi}{2Z_\circ\sqrt{\varepsilon_r}} \tag{2.20}$$

Notice that with the previous equations it is also possible to calculate the width of the microstrip line. Substrate definition include the ε_r and the h, by stipulating a characteristic impedance for the microstrip line will give access for the width calculation of the microstrip line. Due to this propagation method the wavelength in a microstrip medium is given by:

$$\lambda_g = \frac{\lambda_\circ}{\sqrt{\varepsilon_{eff}}} \tag{2.21}$$

Considering two points in the same transmission line separated by one wavelength we can say that they have a phase difference of 2π. With this it becomes possible to determine the wavelength along the transmission line:

$$wt - \beta z = wt - \beta(z + \lambda) + 2\pi \leftrightarrow$$

$$\leftrightarrow 0 = -\beta\lambda + 2\pi \leftrightarrow \beta\lambda = 2\pi \leftrightarrow$$

$$\leftrightarrow \lambda = \frac{2\pi}{\beta} \tag{2.22}$$

Meanwhile, velocity of propagation (v_p) can be expressed by the wavelength along the transmission line at the operation frequency:

$$v_p = f\lambda \tag{2.23}$$

$$v_p = \frac{w}{\beta} \tag{2.24}$$

Using Eq. (2.6):

$$v_p = \frac{1}{\sqrt{LC}} \tag{2.25}$$

The capacitance of a line that is uniformly filled with dielectric material is proportional to ε_r. And the velocity in an air-filled transmission line is approximately the velocity of light in free space, so:

$$v_p = \frac{c}{\sqrt{\varepsilon_r}} \; {}^m/_s \tag{2.26}$$

The total voltage and current of the line is a superposition of the incident and the reflected wave (standing waves). The voltage reflection coefficient is defined as the ratio of the amplitude of the reflected voltage by the amplitude of the incident voltage:

$$\Gamma = \frac{V_\circ^-}{V_\circ^+} = \frac{Z_L - Z_\circ}{Z_L + Z_\circ} \tag{2.27}$$
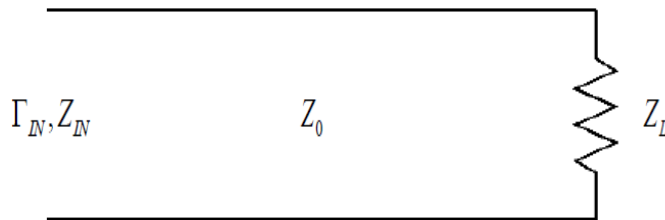

Figure 3: Transmission line with load termination

When $\Gamma = 0$, there is no reflected wave. In order to achieve $\Gamma = 0$, the load impedance Z_L must be equal to $Z_\circ$. In this case the load is matched to the line, since there is no reflection of the incident wave.

When $Z_L \neq Z_\circ$ (mismatch), the line voltage magnitude V_{max} is not constant and this voltage V_{min} magnitude will oscillate along the line. The ratio of maximum voltage magnitude to the minimum voltage magnitude is defined as the Voltage Standing Wave Ratio(VSWR).

$$VSWR = \frac{V_{max}}{V_{min}} = \frac{1 + |\Gamma|}{1 - |\Gamma|} \tag{2.28}$$

The input impedance of a lossless transmission line with length $l = \lambda/2$, propagation constant β and characteristic impedance $Z_\circ$, terminated by arbitrary load impedance Z_L is given as:

$$Z_{in} = Z_\circ \frac{Z_L + jZ_\circ tan\beta l}{Z_\circ + jZ_L tan\beta l} \tag{2.29}$$

The electrical length (βl) is normally given in degrees. If there is a short circuit in the line then $Z_L = 0$ and from Eq. (2.29) as:

$$Z_{sc} = jZ_\circ tan\beta l \tag{2.30}$$

When $Z_L = \infty$ (open circuit), using Eq. (2.26) the input impedance is:

$$Z_{oc} = - jZ_\circ cot\beta l \tag{2.31}$$

2.3.3. Lossless Terminated Lines (short and open circuit transmission lines)

How transmission lines are terminated is an important issue in practical designs. Consider a line terminated by a short circuit as follows:
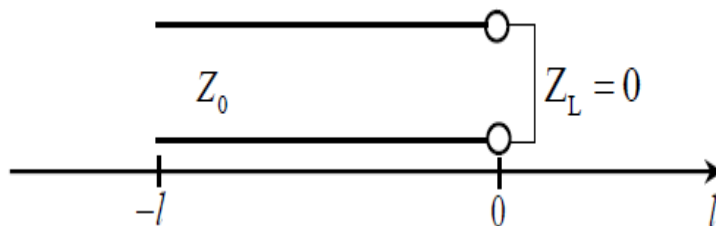
Figure 4: Short-circuited transmission line

One very important issue to consider regarding a transmission line is its impedance. And the impedance of a short circuit line has the following behavior as:
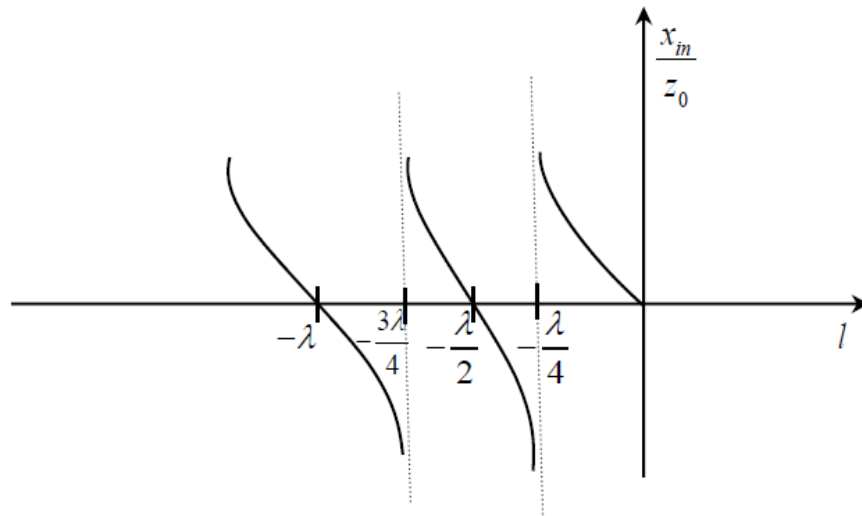
Figure 5: Impedance behavior along a short circuit transmission line

For $l = 0 \rightarrow z_{in} = 0$, however, for $l = \frac{\lambda}{4} \rightarrow z_{in} = \infty$ (open circuit). So, it is periodic in multiples of $\lambda/2$[17]. For $l < \lambda/4$ the line becomes inductive, and for $\lambda/4 < l < \lambda/2$ it shows a capacitive response [25].

An open circuit terminated line is illustrated in Figure 6.
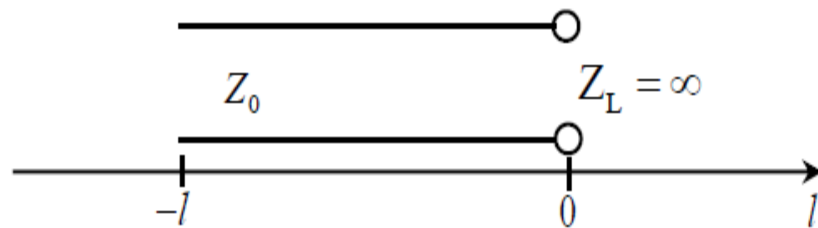
Figure 6: Open-circuited transmission line

Also, the impedance behavior along an open circuit line is given by Figure 7.
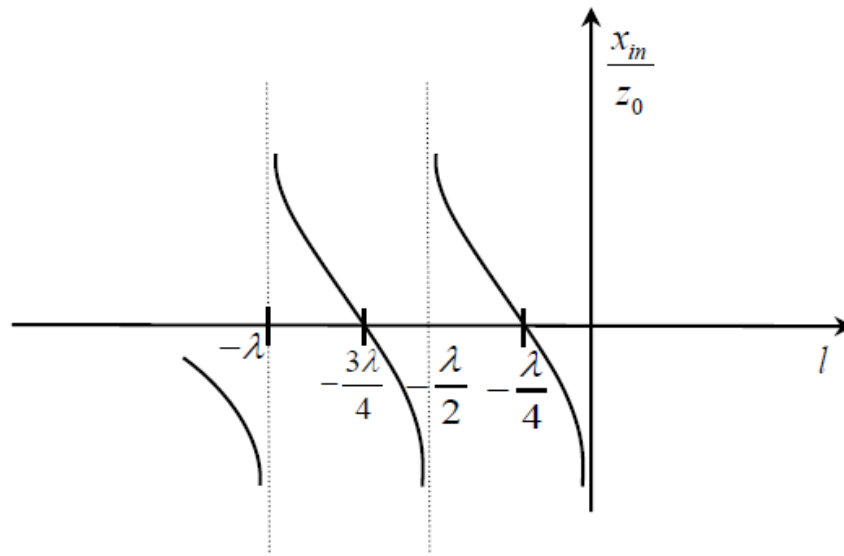
Figure 7: Impedance behavior along an open circuit transmission line

Notice that any multiple of $\lambda/2$ does not change the load impedance as seen above. However, if the transmission line is a quarter wavelength length long, or it can be written as $l = \lambda/4 + n\lambda/2$ with n=1,2,3… it will transform/invert the load impedance [17].

For $l < \lambda/4$ the line has a capacitive behavior, and for $\lambda/4 < l < \lambda/2$ it shows an inductive response[25]. As seen, passive circuit elements can be represented by short-circuited or open circuited lines. If an open-circuit is proposed, for different length values the correspondent circuits are illustrated in Figure 8.
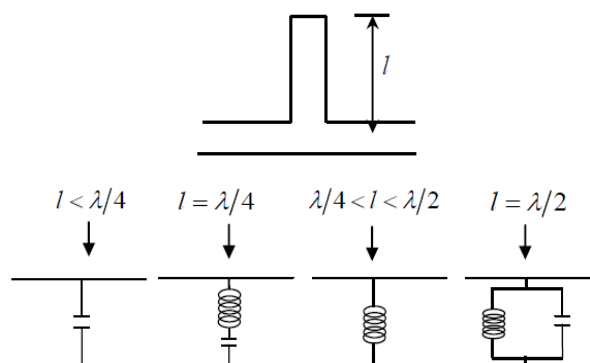
Figure 8: Representation of capacitance and inductance of microstrip lines [26]

If a short circuit line is used then length variation presents the following behaviors:
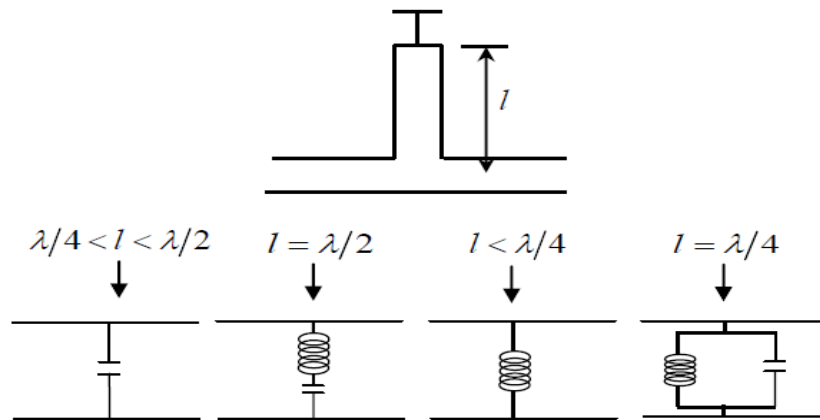
Figure 9: Inductive and capacitive reactance example in microstrip line [26]

Thus, for different lengths values different behaviors will occur. This methodology is also used for line series resonant circuits as seen in Figure 10.
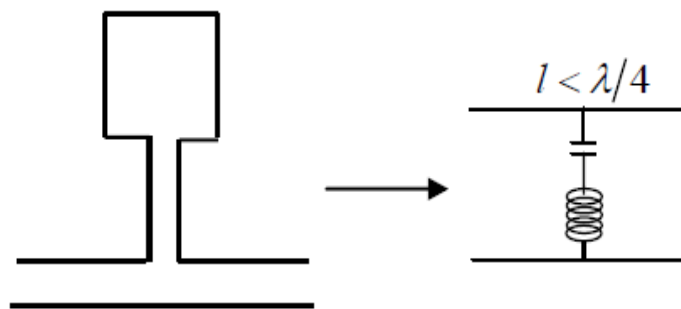
Figure 10: Inductive and capacitive reactance example in microstrip line [26]

2.3.4. Discontinuities

Transmission lines present several types of discontinuities. Sometimes discontinuities results from mechanical or electrical transitions from one medium to another. Normally the effect of discontinuity is seen as an undesirable event, however, sometimes discontinuities are deliberately implemented into the circuit in order to provide a certain electrical function. Either way, the discontinuities can be represented by an equivalent circuit. For this purpose usually the T or Π equivalent circuit is used [17].

Common microstrip discontinuities are the open ended that consist on a line over the substrate that which produces capacitor behavior as illustrated in Figure 11.
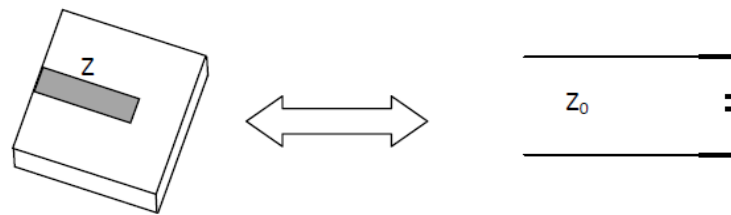
Figure 11: Open-ended discontinuity

The Gap discontinuity consists in two lines with open ended behaviors plus the additional coupling effect between them both as exemplified in Figure 12:
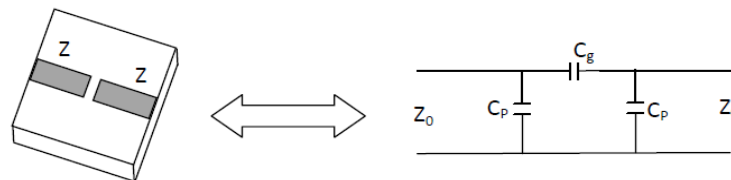
Figure 12: Gap discontinuity

When different line sections have different width values then discontinuities effects appear in the circuit as well. Notice that common microstrip structures are based on this oscillating effect such as lowpass filters. This event can be characterized with Figure 13 circuit [17].
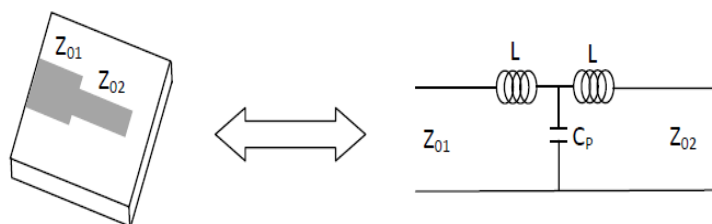
Figure 13: Change in width discontinuity

Discontinuities at bends, step changes in widths and junctions cause degradations in circuit performance. These discontinuities introduce parasitic reactance that can lead to phase and amplitude errors, input or output mismatch and other undesirable effects. As seen, one approach is to include an additional circuit to adjust the circuit performance. However, another approach can be taken. It consists on minimizing the

effect of the discontinuities by slightly modifying the design structure. Consider Figure 14.

Figure 14: Bend effect

The right angle has a parasitic discontinuity capacitance caused by the increased conductor area near the bend. To eliminate this effect it is made a smooth bend with radius $r \geq 3w$ or a slice of the corner must be taken off. This will reduce the excess capacitance of the bend (Figure 15). The optimums bend value depends on the characteristic impedance and the angle, so a miter length equal to 8 times the frequency used is a reasonable bend [17].
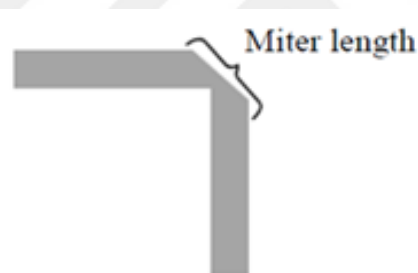
Figure 15: Mitering the bend

2.3.5. Stub Tuning

Stub tuning is a matching technique that uses open-circuit or short-circuits length of transmission line connected at a curtained distance from the load. There are two important parameters to take into account with this methodology, i.e. the distance from the load and the value of reactance provided by the stub [17]. For practical consideration this method optimizes the circuit response and brings it back to zero.

2.4. Scattering Matrix

In microwave frequencies the idea of voltage, current and impedances is less descriptive when high networks are analyzed. Instead, an analysis of incident and reflected waves is used.

The scattering matrix provides a good and complete description of a high frequency network as seen by its N ports, in terms of incident/reflected voltage travelling waves. For this matter this matrix becomes a valuable tool to evaluate per example the filters performance. *S*-parameters can be measured by a network analyzer or calculated using network analysis techniques [17].
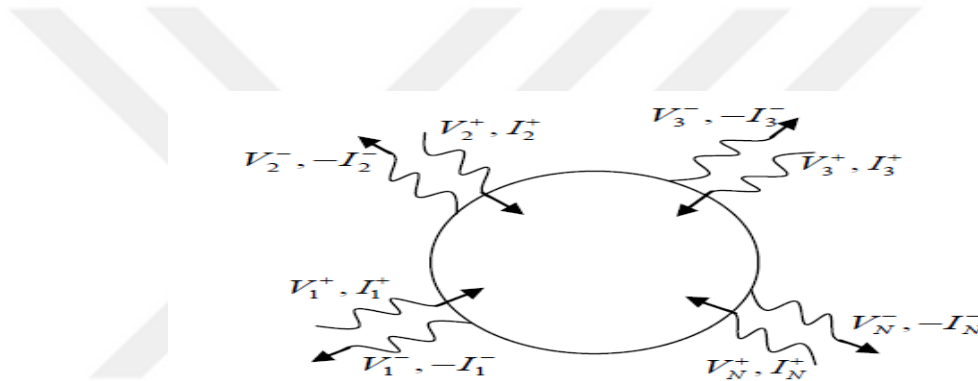
Figure 16: N-port microwave network

As seen in Figure 16, the V_n^+ is the amplitude of the incident voltage wave on port n and V_n^- is the amplitude of the reflected wave from port n. The scattering matrix $[S]$ is defined as:

$$
\begin{bmatrix} V_1^- \\ V_2^- \\ \vdots \\ \vdots \\ \vdots \\ V_N^- \end{bmatrix} = \begin{bmatrix} S_{11} & S_{12} & \cdots & & \cdots & S_{1N} \\ S_{21} & S_{22} & \cdots & & \cdots & S_{2N} \\ \vdots & \vdots & & & & \vdots \\ \vdots & \vdots & & & & \\ \vdots & \vdots & & & \vdots & \\ S_{N1} & S_{N2} & \vdots & \vdots & \vdots & S_{NN} \end{bmatrix} \begin{bmatrix} V_1^+ \\ V_2^+ \\ \vdots \\ \vdots \\ \vdots \\ V_N^+ \end{bmatrix} \tag{2.32}
$$

An element of the matrix $[S]$ is defined as:

$$S_{ij} = \frac{V_i^-}{V_j^+}\bigg|_{V_k^+ = 0 \, for \, k \neq j}$$

(2.33)

Meaning that S_{ij} (transmission coefficient) can be found by putting through port j an incident voltage wave of amplitude V_j^+ and measuring the reflected wave amplitude V_j^- from port i. To avoid reflections all ports except port j should terminate in matched loads. In the same manner S_{ii} is the reflection coefficient seen through port i when all other ports are terminated in matched loads [17].

Consider a two port network. If we want to measure S_{11}, we inject a signal at port one and measure its reflected signal. In practical experiments it is advised to only inject one signal at a time. If measuring S_{21}, it is injected a signal at port 1, and then the resulting signal existing at port 2 is measured. For S_{12} a signal is injected into port 2, and measured in the leaving port 1, and for S_{22} it is injected a signal at port 2 and the reflected signal is measured at port 2 as well [27].

2.5. ABCD Parameters

A large group of microwave networks consist of a cascade connection of two or more two-port networks. When this happens it is defined a 2x2 transmission or ABCD matrix for each two-port network. The ABCD matrix is defined by:

$$V_1 = AV_2 + BI_2$$

(2.34)

$$I_1 = CV_2 + DI_2$$

(2.35)

$$\begin{bmatrix} V_1 \\ I_1 \end{bmatrix} = \begin{bmatrix} A & B \\ C & D \end{bmatrix} \begin{bmatrix} V_2 \\ I_2 \end{bmatrix}$$

(2.36)

These equations represent the following system:
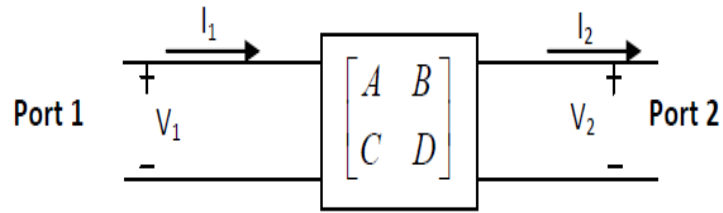
Figure 17: ABCD system

Looking at the cascade network:
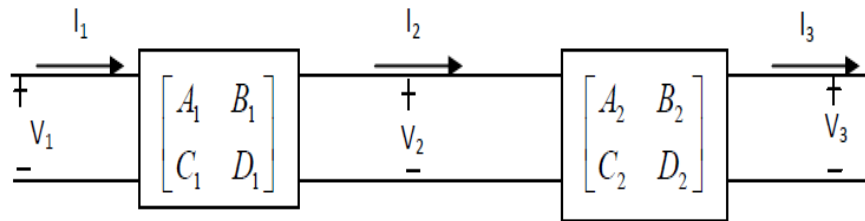
Figure 18: Cascade network example

Which means that ABCD matrix of the cascade connection is equal to the product of the ABCD matrices representing individual ports.

$$\begin{bmatrix} V_1 \\ I_1 \end{bmatrix} = \begin{bmatrix} A_1 & B_1 \\ C_1 & D_1 \end{bmatrix} \begin{bmatrix} A_2 & B_2 \\ C_2 & D_2 \end{bmatrix} \begin{bmatrix} V_3 \\ I_3 \end{bmatrix} \tag{2.37}$$

This is a useful method when a more complicated microwave network that consists of cascades of this simpler two-ports need to be analyzed [17].

2.6. Richard's Transformation

Richard's transformation equals the behavior of lumped elements (L or C) and a given stub with respective characteristic impedance and length at precisely one frequency as illustrated in Figure 19. The input impedance of short and open circuit transmission lines is given by Eq. (2.30) and Eq.(2.31). However, transmission line stubs mathematically differs from the reactance of lumped inductors and capacitors as seen in equations:

$$Z_L = jwL \tag{2.38}$$

$$Z_C = \frac{-j}{wC} \qquad (2.39)$$

Meaning that the impedances of transmission line stubs and lumped elements differ regarding its frequency, which leads to the following:

$$Z_{IN}^S \neq Z_L \qquad (2.40)$$

$$Z_{IN}^O \neq Z_C \qquad (2.41)$$

Where Z_{IN}^S is the input short circuit transmission line impedance and Z_{IN}^O refers to the open circuit transmission line impedance. On the other hand, if a single frequency is used than these functions will equalize and a transformation can be developed. So, if a frequency (w_C) satisfies the following equation:

$$jw_C = jZ_0 tan\beta_C l \leftrightarrow$$

$$= jZ_0 \tan\left[\frac{w_C}{v_p} l\right] \qquad (2.42)$$

Or similarly in the lumped capacitor case:

$$\frac{-j}{w_C C} = jZ_0 cot\beta_C l \leftrightarrow$$

$$= -jZ_0 cot\left[\frac{w_C}{v_p} l\right] \qquad (2.43)$$

Assuming a stub transmission length of $\lambda/8$ and Eq. (2.22) the following wavelength is achieved:

$$\lambda_C = \frac{v_p}{w_C} = \frac{2\pi}{\beta_C} \qquad (2.44)$$

Eq. (2.30) will achieve the following expression:

$$jw_C = jZ_0 tan\beta_C l = jZ_0 \tan\left[\frac{\pi}{4}\right] = jZ_0 \qquad (2.45)$$

Similarly, Eq. (2.31) acquires the referred expression:

$$\frac{-j}{w_C C} = jZ_0 cot\beta_C l = -jZ_0 \qquad (2.46)$$

A short circuit stub with the same impedance as an inductor L at frequency w_C can be achieved if the characteristic impedance of the stub is set to $w_C L$. Likewise an open circuit stub can be designed if his characteristic impedance has the value $\frac{1}{w_C L}$.

Richard Transformations:
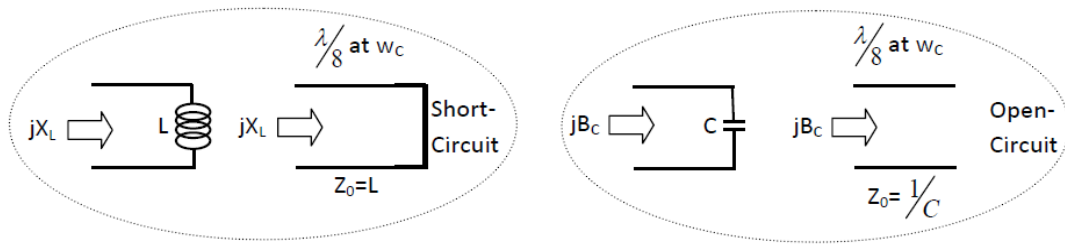
Figure 19:Richard Transformations

Richard's Transformations do not result in perfect replacements for lumped elements i.e. the stubs do not behave like capacitors and inductors. What happens is that the transformation is perfect and impedances are equal at a certain frequency w_C. This w_C is also known as the cutoff frequency of a lumped element filter design whose inductors and capacitances were replaced by Richard's transformations [17].

2.7. Kurodas's Identities

The four Kuroda identities utilize outmoded transmission line sections to allow implementation of microwave filters. They take apart transmission line stubs, transforms series stubs into shunt stubs and vice-versa and replaces characteristic impedances that are difficult to implement with more practical ones. The further transmission line segments are known as unit elements and are $\lambda/8$ long at the cutoff

frequency and they are commensurate (all lengths of all the stubs are the same) with the stubs that realize the inductors and capacitors of the prototype design. The four identities within each specific box representing a unit element (transmission line) of the specified characteristic impedance and length $\lambda/8$ at w_c areexisting in Ref. [17]. For every identity the equivalence between the two networks can be proved demonstrating that their $ABCD$ matrices are equal [17].

2.8. Filtering

A filter is a frequency selective device that is used to bound the signal spectrum to some particular band of frequencies. Its frequency response is described by the properties of passband and stopband. The frequencies inside the passband are sent with low level or no distortion, while those in the stopband are discarded. The filter can be of lowpass, highpass or bandstop type.

2.9. Microstrip Filters

The following subsections will introduce the microstrip configurations used to form lowpass and bandpass filters. Microstrip filters design can take many forms. A useful one is achieved by using classical filter prototypes and changing them to the microstrip by using the equivalent short lengths of transmission line to inductance or capacitance.

2.10. Lowpass Filters

Lumped elements, capacitors and inductors, in microwave filters normally have a partial range of availability, and therefore are very difficult to implement inmicrowave frequencies. Plus the distances among filter components can be a problem. To overcome these barriers Richard's transformation has the possibility to adapt lumped elements to transmission line sections and Kuroda's identities to specifically separate filter elements using transmission line sections. These sections are often used to improve filters response once their inclusions do not affect the filter response (redundant filter synthesis).

2.10.1. Stepped-Impedance Methodology

The stepped-impedance method illustrated in Figure 20, consists of alternating section with very high and very low characteristics impedances. This method has the advantage of being relatively easy to build. Additionally, it takes less space than a similar lowpass filter using stubs. The disadvantage is the electrical performance. This method of construction is often indicated to applications were a sharp cutoff frequency is not required. More specifically because of the radiations, transverse resonances and other undesirable effects, the stepped-impedance method is not suitable for microwave frequencies higher than 20 *GHz*. However, bellow 20 *GHz*, with the actual technologies and simulators available to engineers this disadvantage becomes a minor issue.
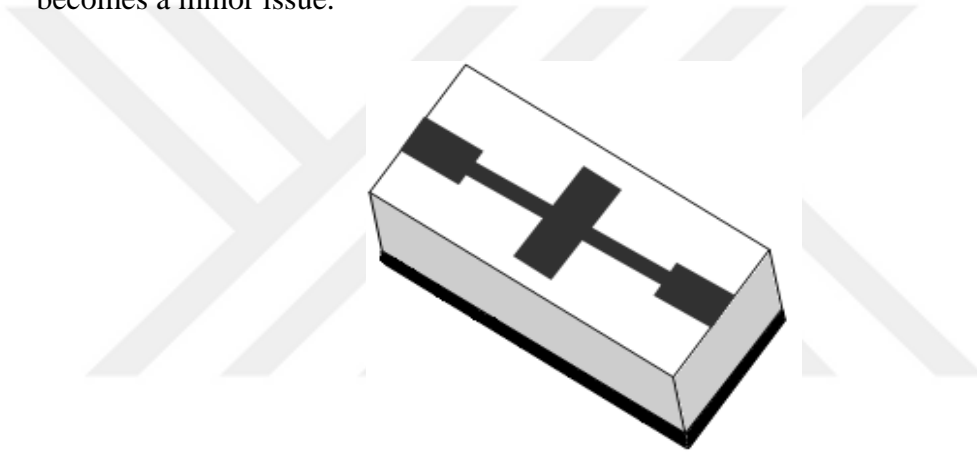
Figure 20: Lowpass microstrip filter using stepped-impedance method

The main idea is to find the *T*-equivalent circuit for a short length of transmission line (electrical length $\beta l \ll \pi/2$) with either very large or very small characteristic impedance (Figure 21).
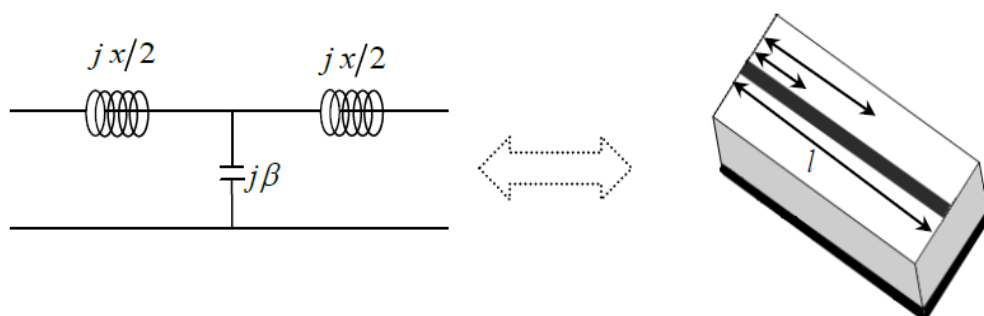
Figure 21: T-equivalent circuit for a short length transmission line

Regarding the cases where large characteristic impedance exist the T-equivalent circuit transforms itself to a series inductor (Figure 22). On the other hand if the transmission medium has small characteristic impedance then the T-equivalent reduces to a shunt capacitor (Figure 23).
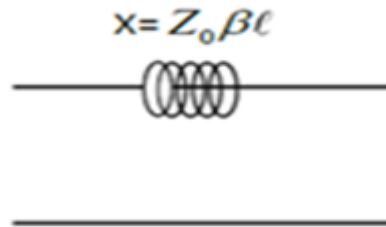
Figure 22: High characteristic impedance circuit equivalent
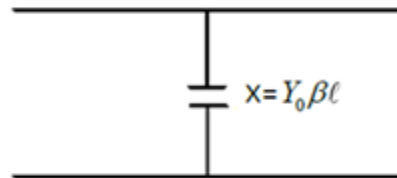
Figure 23: Low characteristic impedance circuit equivalent

These high and small impedances lines into the prototype will produce the final ladder configuration (see Figure 20). It is proved that the ratio between the highest and lowest characteristic impedance should be in the interval 9-200 Ω [28]. However, in reality these values cannot be followed, and instead of this relation, an optimum value is discovered based on the substrate and its specific characteristics.

2.10.2. Lowpass Realization

Normally lowpass filters are implemented using lumped elements such as capacitors, resistors and inductors. It is common to use two syntheses techniques:

- **Image-Parameter Method (IPM)**

The purpose of this method is to design high-order filters with reasonable performances [29]. It divides the filter into a cascade of two port networks and discovers the schematic of each two-port. Finally, it combines each port and gives the required frequency response [30]

The passband and stopband characteristic for a cascade of two port networks have to be specified. This is helpful for undemanding filters and it provides a link between infinitive periodic structures and practical filter design [17]. This method has the disadvantage that an arbitrary frequency response cannot be incorporated in the design and at the same time if a good filter response is not succeeded there is no direct way to improve the design.

- **Insertion-Loss Method (ILM)**

An arbitrary frequency response can be incorporated into the design with the Insertion Loss method. ILM permits an elevated degree of control over the passband and stopband amplitude and also over phase characteristics. This is done in a very systematic approach and pointing down to the user desired response. For example, if the goal is to have the minimum insertion loss possible then a binomial response could be used, or if the goal is to obtain the sharpest cutoff then chebyshev would the chosen. This method has a direct relation with the filters order which equals the number of reactive elements in the circuit [17]. The design procedure of the Insertion Loss (IL) method is based on the attenuation response (insertion loss) of the filter:

$$IL = \frac{Source\ Power}{Load\ Power} = \frac{1}{1 - |\Gamma(w)|^2} \qquad (2.47)$$

Where Γ is the reflection coefficient when looking into the filter. To follow this method it is necessary to design a normalized lowpass prototype (LPP). This prototype consists on several connected reactive elements as illustrated in Figure 24. Afterwards, impedance transformations and frequency scaling are applied to transform the LPP.
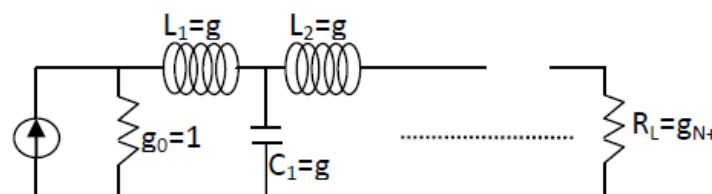
Figure 24: Lowpass filter prototype

The order of this ladder network (Figure 24) corresponds to the number of reactive elements. The goal is to approximate the ideal amplitude response of an amplifier ($|H(\omega)|^2$) using polynomials such as Butterworth, Chebyshev, etc.

Consider the following schematic and equation for the amplitude response discussed:
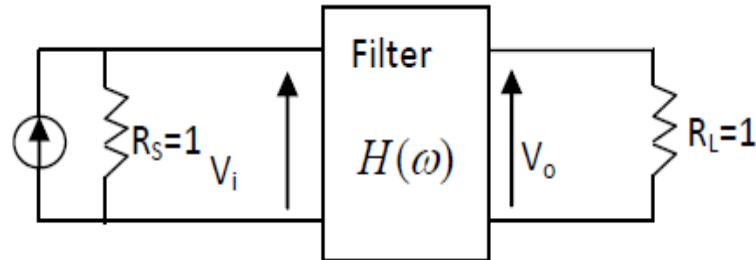
Figure 25: LPP for amplitude response calculation

$$H(\omega) = \frac{V_\circ(\omega)}{V_i(\omega)} = \frac{K_\circ}{1 + C_\circ P_N(\omega)} \tag{2.48}$$

In this equation $K_\circ$ and $C_\circ$ are constants that depend on the polynomial used and is a $P_N(\omega)$ polynomial in ω of order N. Regarding the polynomials choice there are some important issues to take into account. Chebyshev provides rapid cut off frequency, Bessel provides the slowest cut off frequency, and Butterworth's response remains between them. Butterworth is also known for its flattest response. After choosing the appropriate polynomial the respective inductance and capacitance can be obtained. This is done regarding a specific order and referring to tabulated values presented by several authors [17]. There are alternative approaches than can be seen in [31-32]. If we want to achieve a maximally flat response than the tabulated values of the respective LPP are the following Ref. [33]:

Table 1: Element values for the maximally flat lowpass filter prototypes [17]

N	g_1	g_2	g_3	g_4	g_5	g_6	g_7	g_8	g_9	g_{10}	g_{11}
1	2.0000	1.0000									
2	1.4142	1.4142	1.0000								
3	1.0000	2.0000	1.0000	1.0000							
4	0.7654	1.8478	1.8478	0.7654	1.0000						
5	0.6180	1.6180	2.0000	1.6180	0.6180	1.0000					
6	0.5176	1.4142	1.9318	1.9318	1.4142	0.5176	1.0000				
7	0.4450	1.2470	1.8019	2.0000	1.8019	1.2470	0.4450	1.0000			
8	0.3902	1.1111	1.6629	1.9615	1.9615	1.6629	1.1111	0.3902	1.0000		
9	0.3473	1.0000	1.5321	1.8794	2.0000	1.8794	1.5321	1.0000	0.3473	1.0000	
10	0.3129	0.9080	1.4142	1.7820	1.9754	1.9754	1.7820	1.4142	0.9080	0.3129	1.0000

The letter g represents the lowpass prototype element values for each filter order. After creating the specified LPP filter and attributing the correct above elements an impedance and frequency scaling must be performed. Therefore a new load impedance, cutoff frequency, resistance, capacitance and inductance are changed by the following expressions in order to transform de circuit:

$$R = R_0 R_n \tag{2.48}$$

$$L = R_0 \frac{L_n}{W_0} \tag{2.49}$$

$$C = \frac{C_n}{R_0 W_0} \tag{2.50}$$

Scaling impedances means multiplying each impedance by R_0. On the other hand, frequency scaling is achieved with $w_n = w/w_0$. If a capacitor C is replaced with C/w_0 its frequency response is also scaled by w_0. However, the resistor is not affected by frequency scaling because it is frequency independent. After an appropriate impedance and frequency scaling the new elements are given by Eq. (2.51) and Eq. (2.52) [17]:

$$L_k = \frac{R_0 g_k}{\omega_c} \tag{2.51}$$

$$C_k = \frac{g_k}{R_0 \omega_c} \tag{2.52}$$

The circuit of the stepped-impedance method scaled will have this form:
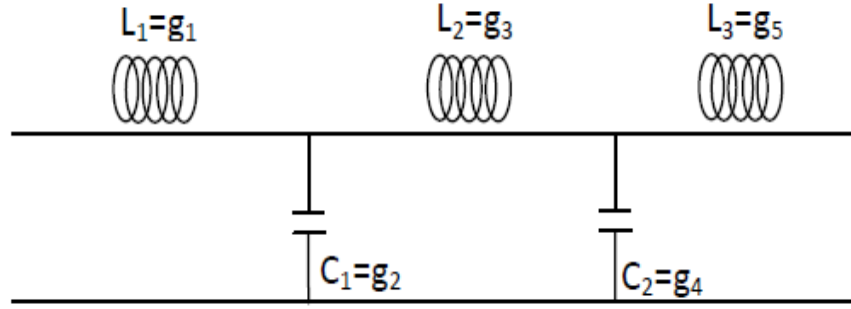
Figure 26: Stepped impedance method

The final correspondent microstrip layout will have the following appearance:
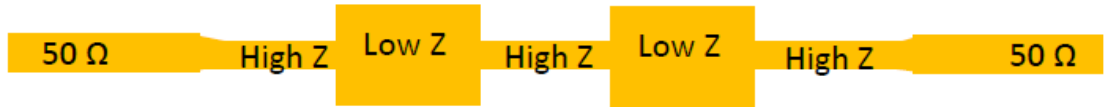
Figure 27 Layout of a microstrip stepped impedance circuit

A good substrate choice must be made due to the electrical performance desired, length of the circuit, price and circuit stability. To obtain this layout the effective permittivity, width and length must be found. For a better analysis and due to the fringing fields at the end of the low impedance line sections the inclusion of a T-equivalentcircuit maybe considered for these sections or/and an interactive approach correcting the modified initial design can be taken into account. So, the length for a high impedance line (or in terms of the required inductance) is given by:

$$l = \frac{\lambda_H}{2\pi} sin^{-1}\left(\frac{wL_k}{Z_H}\right) \tag{2.53}$$

With the two shunt-capacitances elements:

$$C_L = \frac{1}{wZ_H} \tan\left(\frac{\pi l}{\lambda_H}\right) \tag{2.54}$$

Where λ_H and Z_H are the wavelength and characteristic impedance associated with the high impedance microstrip line. As for the low impedance line the methodology is very similar. The length of the desired capacitance is:

$$l = \frac{\lambda_L}{2\pi} sin^{-1}(wC_kZ_L) \tag{2.55}$$

Also, the series inductances are given by:

$$L_C = \frac{Z_L}{w} \tan\left(\frac{\pi l}{\lambda_L}\right) \tag{2.56}$$

An interactive process is used until a good stable solution is found [23], i.e. the initial element length is found and the initial values are modified regarding the fringing capacitances of the high impedance lines and the inductive components of the low impedance lines. The width is found by considering the substrate used (dielectric and thickness) and the line characteristic impedance as indicated in Eq.(2.16) and Eq.(2.17).

2.11. Bandpass Filters

The design of bandpass filters starts with the design of a prototype lowpass filter with the required passband and attenuation characteristics. Once a prototype is available it ispossible to transform the values using simple algebraic identities to give high-pass and bandpass filters with the same shape.The mapping from the lowpass prototype response (Butterworth) to the bandpass response is shown in Figure 28.
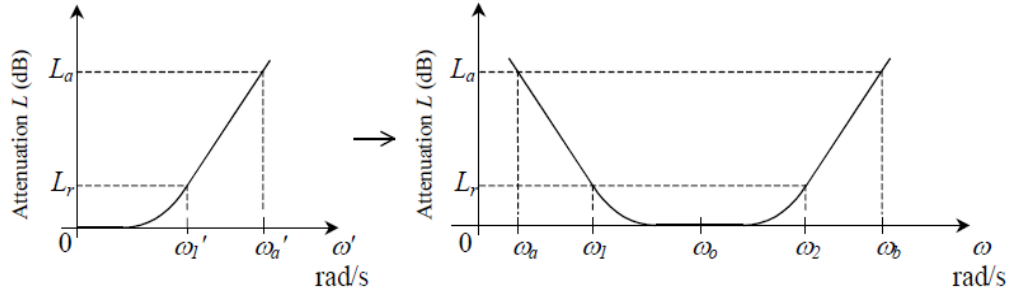
Figure 28:Corresponding bandpass filter response regarding the Butterworth lowpass filter response

All elements of the lowpass prototype are replaced by tuned circuits i.e. inductors are replaced by series L-C tuned resonant circuits and capacitors are replaced by parallel L-C tuned resonant circuits. The lowpass prototype values g_k of an nth order filter are given by [33]:

$$g_k = 2 \sin\left(\frac{(2k-1)\pi}{2n}\right) \tag{2.57}$$

The previous equation refers to maximally flat filters (Butterworth), with $g_0 = g_n + 1 = 1.0$ and attenuation $L_r = 3dB$ at $\omega_1' = 1$ rad/s.

The transformation from lowpass filter to bandpass filter can be expressed as:

$$\frac{\omega'}{\omega_1'} = \frac{1}{\Delta}\left(\frac{\omega}{\omega_o} - \frac{\omega_o}{\omega}\right) = \frac{1}{\Delta}\left(\frac{f}{f_0} - \frac{f_0}{f}\right) \tag{2.58}$$

where Δ is the 3 dB fractional bandwidth and ω_o is the centre frequency of the bandpass filter and are given by:

$$\Delta = \frac{\omega_2 - \omega_1}{\omega_o} = \frac{f_2 - f_1}{f_0} \tag{2.59}$$

$$\omega_o = \sqrt{\omega_2 \omega_1} \tag{2.60}$$

An important issue is that multiple resonances exist in a transmission line resonator resulting in additional higher frequency passbands (*spurious passbands*) that are not predictedby Eq. (2.58). For broadband filter design it is necessary to use mapping functions that predict more accurately the frequency response.

34

For odd (Z_{0o}) and even (Z_{0e}) mode line impedance calculations it is considered a quarter wave length (λ/4) transmission line section with $1/J$ of characteristic impedance [17]:

$$Z_{0o} = Z_0(1 - JZ_0 + (JZ_0)^2) \qquad (2.61)$$

$$Z_{0e} = Z_0(1 + JZ_0 + (JZ_0)^2) \qquad (2.62)$$

Note that Z_0 is the characteristic impedance of the input and output connecting lines. A bandpass filter with three cascaded coupled line sections is illustrated in Figure 29.
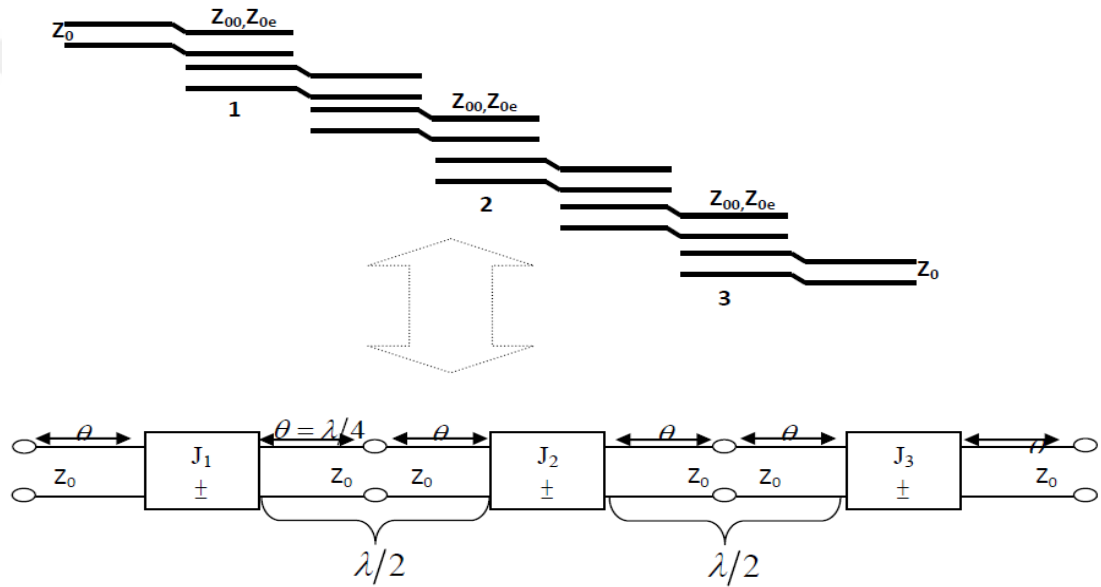
Figure 29:Bandpass cascade with 3 coupled line sections equivalent [23]

This circuit can also be equivalent to a lumped elements circuit [17].Between the consecutive inverters we have a transmission line section that has 2θ in length which makes it $\lambda/2$ between sections as illustrated above. They also act as resonators due to the $\lambda/4$ lines attached to the inverters.Considering the elements (inductors or capacitors) of this prototype filter as $g_0, g_1, \ldots \ldots, g_N$, and that Δ corresponds to the $3dB$ fractional bandwidth, from reference [17], the normalized admittance parameters are calculated through:

$$Z_0 J_1 = \sqrt{\frac{\pi\Delta}{2g_0 g_1}} \qquad (2.63)$$

$$Z_0 J_N = \frac{\pi \Delta}{2\sqrt{g_{N-1} g_N}} \quad , n = 2, \ldots \ldots \ldots N \tag{2.64}$$

$$Z_0 J_{N+1} = \sqrt{\frac{\pi \Delta}{2 g_N \, g_{N+1}}} \tag{2.65}$$

After this, the even and odd line impedances may be calculated through Eq.(2.61) and Eq.(2.62).

2.11.1. Bandpass Filter Structures

The three common parallel-coupled microstrip structures each representing a 4th order bandpass filter are illustrated below.
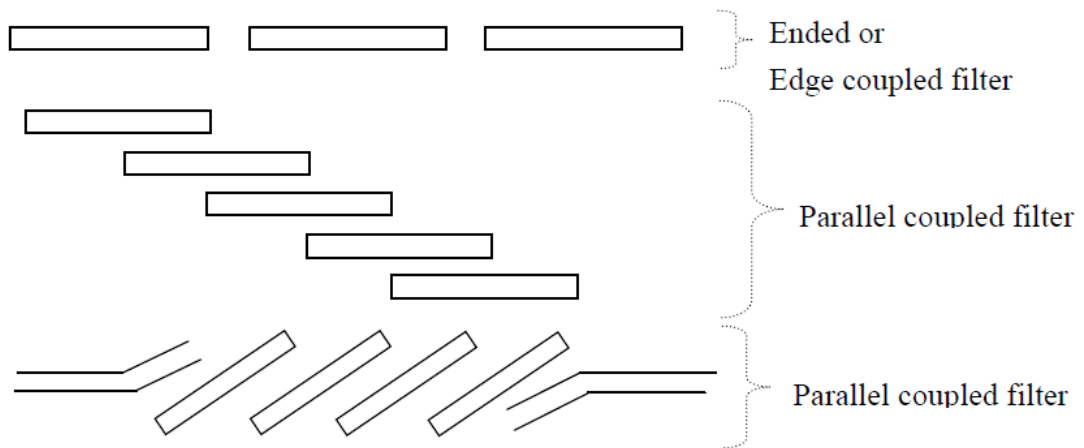
Figure 30: Couple resonator bandpass filters

One usual way to represent bandpass filters is to use parallel coupled microstrip structures.

The advantages from Parallel coupled filters over end coupled are [34]:

- Length (approximately half the size) of the filter.
- Symmetry in frequency response is obtained at three times the center frequency, larger gap supported between adjacent microstrips.

CHAPTER 3

MICROSTRIP RING RESONATORS

3.1. Introduction

Microstrip ring resonators have been considered widely for many applications, such as, compact antennas and dual-mode filters. The first definition of it as a field theory was occurred by Wolff and Knoppik [35], where the magnetic-wall model was well suited to study the curvature effect on the resonant frequency of the ring resonator. Based on magnetic-wall technique, the technique chart for ring resonators, relating the resonant frequency to the ring width and its mean circumference was found by Wu and Rosenbaum [36]. In Ref. [37],by using the eigen-function of Maxwell's equations the frequency modes of the ring resonator were achieved with the boundary conditions of the ring. Mainly, the mode frequencies were found suitable $2\pi r = n\lambda$g, with $n = 1,2,3\dots$, where r is the imply to the radius of the ring resonator, n is the mode number, and λ_g is the guided-wavelength. Hitherto, the theory derivation for its frequency modes can be applied to the annular ring resonator only. Because of the square ring resonator is complex boundary conditions, the application of magnetic wall technique is not easy to get the frequency modes of it. Lately, Hsieh and Chang [38],applied an easy technique to rid from this issue called transmission-line method, which is not related to boundary conditions, by this way the calculation of the frequency mode became easy to be applied in popular forms. This technique has a large-scale application, by applying this technique the dual mode characteristics can be depicted well as compared to magnetic-wall technique, in particular for a square ring resonator with intricate boundary conditions. Moreover, It was applied to elicit the tantamount lumped element circuits for the unsplit-loop and open-loop ring resonators [39].

Various methods have been used to analyze ring resonators [40-41]. In this chapter, we introduce briefly the most common techniques extensively used to characterize microstrip ring resonators. The major limitation of the transmission line method is

the accuracy when treating with a wide strip resonator. In part 3.3, the magnetic-wall model method based on electromagnetic field theory is described. This method abolishes the error since the mean radius approximation in transmission line model. Degenerate modes of the resonator and their excitations are pointed out in Part3.4. Part 3.5 shows the dual-modes of the ring resonator as well as the electric current simulation of the square ring resonator.

3.2. Transmission Line Model of Ring Resonator

Figure 31 describes the construction of the one-port square ring resonator. The entire length l can be shared into l_1 and l_2 portions. This formula is suitable for any common ring shape.
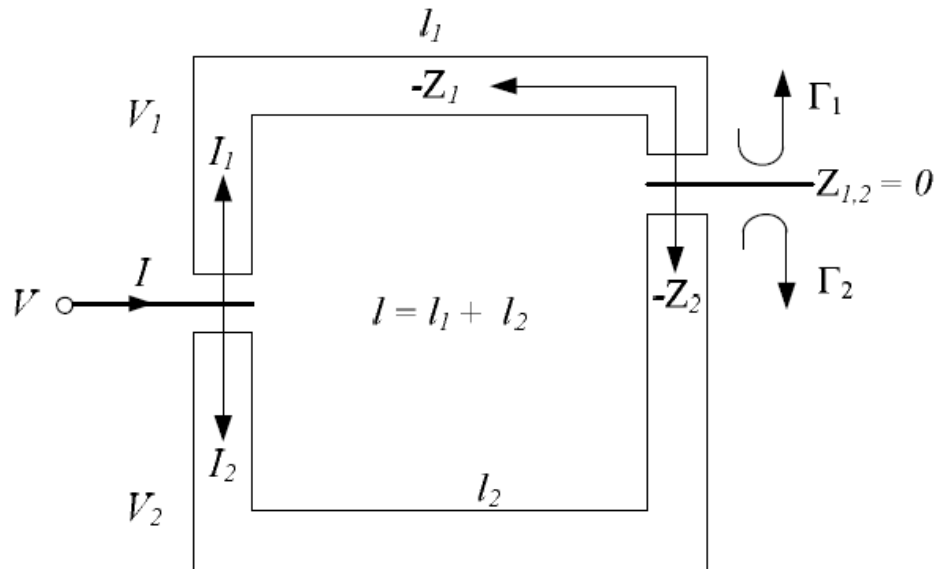
Figure 31: The construction of one-port square ring resonator [38]

In the state of the square ring, each portion is expressed as a transmission line. Z_1 and Z_2 are the coordinates identifying to sequential portions l_1 and l_2. The voltage source (V) supplies the ring at thereabout with $Z_{1,2} < 0$. The locations of the zero site of $Z_{1,2}$ and the voltage (V) are randomly selected on the ring. The equations of the voltages and currents for the two portions in the case of a lossless transmission line are written as follows:

$$V_1(Z_1) = V_\circ^+\left(e^{-j\beta Z_1} + \Gamma_1(0)e^{j\beta Z_1}\right) \tag{3.1a}$$

$$V_2(Z_2) = V_\circ^+\left(e^{-j\beta Z_2} + \Gamma_2(0)e^{j\beta Z_2}\right) \tag{3.1b}$$

$$I_1(Z_1) = \frac{V_\circ^+}{Z_\circ}\left(e^{-j\beta Z_1} - \Gamma_1(0)e^{j\beta Z_1}\right) \tag{3.1c}$$

$$I_2(Z_2) = \frac{V_\circ^+}{Z_\circ}\left(e^{-j\beta Z_2} - \Gamma_2(0)e^{j\beta Z_2}\right) \tag{3.1d}$$

From the equations shown above, the parameters Z_0 and β refer to the characteristic impedance and propagation constant respectively. The reflection of wave propagation $V_\circ^+\Gamma_{1,2}(0)e^{j\beta Z_{1,2}}$ goes to towards the $-Z_{1,2}$ direction, this will be happen when the incident of wave propagation of $V_\circ^+e^{-j\beta Z_{1,2}}$ goes to towards the $+Z_{1,2}$. $\Gamma_{1,2}(0)$ is the reflection coefficient at $Z_{1,2}= 0$. In the case of the resonance, the type of wave, which sends from the ring resonator is called standing wave. The supreme situations values of the standing waves imply the shortest length of ring resonator that props these waves. The absolute values of the peak voltages on the ring resonator can be found as follow[38]:

$$|V_1(Z_1)|_{\max} = 2V_\circ^+ \text{ for } Z_1 = m\frac{\lambda_g}{2}, m = 0, -1, -2, -3, \dots \tag{3.2a}$$

$$|V_2(Z_2)|_{\max} = 2V_\circ^+ \text{ for } Z_2 = m\frac{\lambda_g}{2}, m = 0, -1, -2, -3, \dots \tag{3.2b}$$

Besides, the currents $I_{1,2}$ at the situations of $Z_1 = m\frac{\lambda_g}{2}$ are:

$$I_1(Z_1)\big|_{Z_1=m\frac{\lambda_g}{2}} = I_2(Z_2)\big|_{Z_2=m\frac{\lambda_g}{2}} = 0 \tag{3.3}$$

Moreover, the absolute values of the peak currents can be found [43] as:

$$|I_1(Z_1)|_{\max} = \frac{2V_\circ^+}{Z_\circ} \ for \ Z_1 = \frac{(2m-1)}{4}\lambda_g, m = 0, -1, -2, -3, \dots \tag{3.4a}$$

$$|I_2(Z_2)|_{\max} = \frac{2V_\circ^+}{Z_\circ} \ for \ Z_2 = \frac{(2m-1)}{4}\lambda_g, m = 0, -1, -2, -3, \dots \tag{3.4b}$$

Also, the voltages $V_{1,2}$ at the situations of $Z_{1,2} = \frac{(2m-1)}{4}\lambda_g$ are:

$$V_1(Z_1)\big|_{Z_1 = \frac{(2m-1)}{4}\lambda_g} = V_2(Z_2)\big|_{Z_2 = \frac{(2m-1)}{4}\lambda_g} = 0 \tag{3.5}$$

Figure 32 shows the absolute values of voltage and current standing waves on each part l_1 and l_2 of the square ring resonator. Investigating Figure 32, the standing waves iterate for multiples of $\lambda_g/2$ on the each part of the ring. So, to prop standing waves, the shortest length of each part on the ring has to be $\lambda_g/2$, which can be patronized as the essential mode of the ring. For higher order modes shown in next equation are:

$$l_1 = l_2 = n\frac{\lambda_g}{2}, n = 1, 2, 3, \dots \tag{3.6}$$

Where n refers to mode number. Subsequently, the entire length of the square ring resonator is:

$$l = l_1 + l_2 = n\lambda_g \tag{3.7}$$

The equation written above represents a general case for frequency mode and may be stratified to any shape of microstrip ring resonators such as, the figures as shown in the next page[42-43].
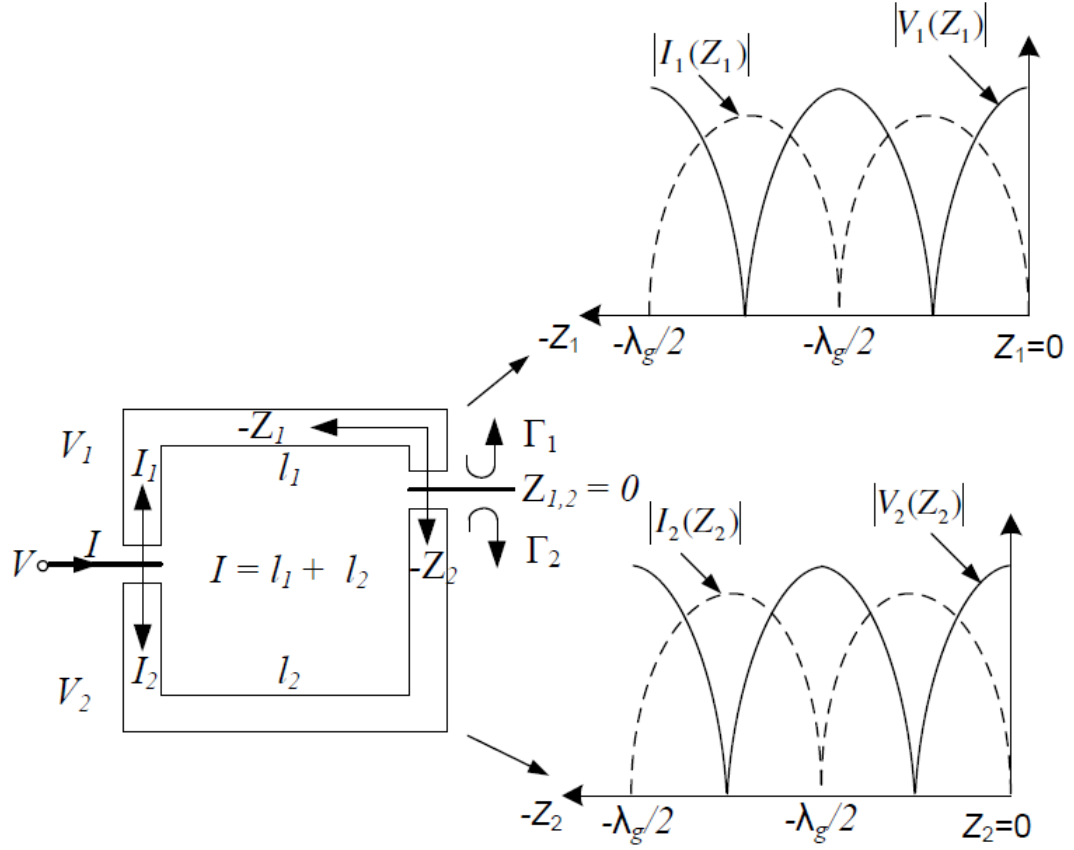
Figure 32: Standing waves on each part of the square ring resonator [38]

Figure 33 appears the geometry of two closed-loop microstrip ring resonators. The straightforward equations of the annularand square rings are given by Eq. (3.8) and Eq. (3.9), respectively

$$2\pi r = n\lambda_g \qquad\qquad (3.8a)$$

$$f_\circ = \frac{nc}{2\pi r\sqrt{\mu_r \varepsilon_{reff}}} \qquad\qquad (3.8b)$$

$$4W = n\lambda_g \qquad\qquad (3.9a)$$

$$f_\circ = \frac{nc}{4W\sqrt{\mu_r \varepsilon_{reff}}} \qquad\qquad (3.9b)$$

Where the f_o refers to the resonant frequency. whereas, λ_g refers to the guided-wavelength, W stands for the length of the square ring, r symbolizes the mean radius

of the annular ring, n is the mode number, c is the speed of light in free space, μ_r is relative permeability, and ε_{reff} is effective relative dielectric constant. Observing these two structures, due to the fact that the line width of the square and annular rings is tight, they have same dispersal traits as a transmission line resonator [44]. Subsequently, the ring resonator can be a unsplit loop transmission line and anatomized by transmission-line technique [45].
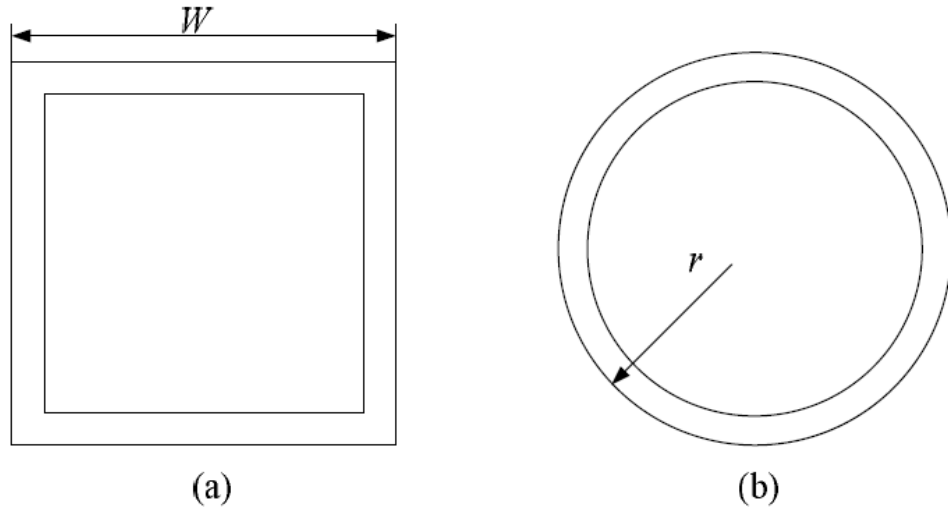
Figure 33:Unsplit-loop microstrip ring resonator (a) Square ring, (b) Annular ring

3.3. Magnetic-Wall Technique of Ring Resonator

This section briefly summarizes the magnetic-wall model that is used to eliminate the mistake because of the average radius approach in transmission line technique, and contains the impact of bend of the microstrip line. This technique for the microstrip ring resonator was explained by Wolff and Knoppik [35]. On the other hand, there was no accurate theory for the resonator for the dispelled impacts on a microstrip line, and the influence of the torsion in a ring resonator unable to clarified by the straight-line approach.

$$2\pi r = n\lambda_g (3.10)$$

Therefore, Wolff and Knoppik [35] made some preparatoryexperiences to quantifythe effects of the torsion on the resonator frequency. There are two important and effective parameters effect oftorsion. The first parameter is that the substrate materials with small relative permittivities (ε_r),and second is that lines with small

impedances. According to the explanation, the widths of the lines willbe large and aaverage radius will notcompletely explained. If small rings are used, then the impacts will be even morestrict due to the amplified torsion [38].
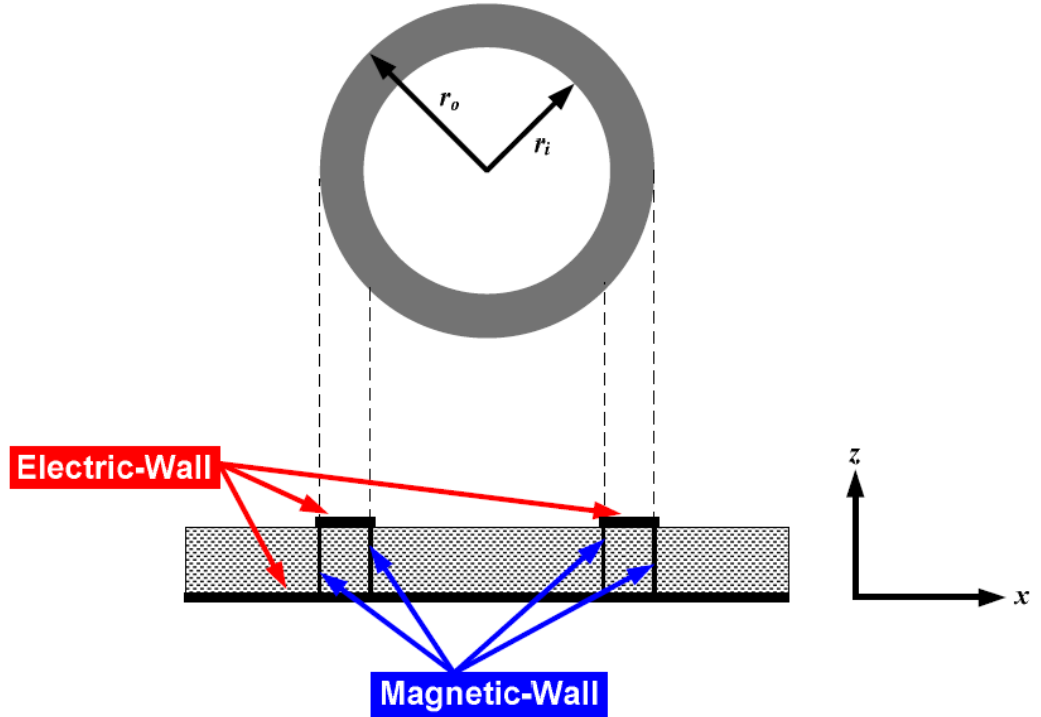
Figure 34: Magnetic-wall model of the ring resonator

This technique considers the ring as a bore resonator with electric walls on the upper and lower, and the magnetic walls on thecylindrical sides of the inner and outer radii of the ring as shown in Figure 34. It is supposed that the z is independent ($\partial/\partial z = 0$) and the fields are transverse magnetic (TM) to z direction [38]. In this case, the solution of Maxwell's equations in cylindrical coordinates is:

$$E_Z = [AJ_n(kr) + BN_n(kr)]\cos(n\emptyset) \qquad (3.11a)$$

$$H_r = \frac{n}{j\omega\mu_\circ r}[AJ_n(kr) + BN_n(kr)]\sin(n\emptyset) \qquad (3.11b)$$

$$H_\emptyset = \frac{n}{j\omega\mu_\circ}[AJ'_n(kr) + BN'_n(kr)]\cos(n\emptyset) \qquad (3.11c)$$

From the equations shown above, both of symbols *A* and *B* imply to constant value, whereas, *k* expresses the number of wave, while ω represents the angular frequency.

The parameters J_n and N_n refer to the Bessel function of the 1st and 2nd type order, respectively. Also, the J_n' and N_n' attribute to the derivatives of the Bessel functions, which are performed according to the argument (kr).

$$H_\emptyset = 0 \quad at \; r = r_\circ$$

$$H_\emptyset = 0 \quad at \; r = r_i$$

By substituting the boundary conditions in Eq. (3.11), it can be found that

$$A J_n'(kr_i) + B N_n'(kr_i) = 0 \tag{3.12a}$$

$$A J_n'(kr_\circ) + B N_n'(kr_\circ) = 0 \tag{3.12b}$$

and this implies to

$$\frac{J_n'(kr_i)}{J_n'(kr_\circ)} = \frac{N_n'(kr_i)}{N_n'(kr_\circ)} \tag{3.13}$$

where $r_\circ$ and r_i are the outer and inner radii of the ring, respectively, and the eigen value equation that can be found by applying the boundary conditions is:

$$J_n'(kr_\circ) N_n'(kr_i) - J_n'(kr_i) N_n'(kr_\circ) = 0 \tag{3.14}$$

Where

$$k = \omega \sqrt{\varepsilon_\circ \varepsilon_r \mu_\circ} \tag{3.15}$$

By using Eq. (3.14) and Eq. (3.15) for given $r_\circ$ and r_i , the resonant frequency $f_\circ$ can be found accordingly.

The resonant modes which are a solution to Eq. (3.14) may be denoted as TM_{nml}, where n is the azimuthal mode number, m is the root number for each n, and $l = 0$ because $\partial/\partial z = 0$. For narrow microstrip widths, as r_i approaches $r_\circ$, Eq. (3.14) can be reduced to

$$[(kr_\circ)^2 - n^2]\{J_{n-1}(kr_\circ)N_n(kr_\circ) - N_{n-1}(kr_\circ)J_n(kr_\circ)\} = 0 \tag{3.15}$$

The second term of Eq. (3.15) is nonzero, and therefore

$$(kr_\circ)^2 - n^2 = 0 \qquad (3.16)$$

Substituting $k = 2\pi / \lambda_g$ into Eq. (3.17) implies to

$$2\pi r_\circ = n\lambda_g \qquad (3.17)$$

which gives the resonances of the TM_{n10} modes and the dominant mode is TM_{110} [36-38].The employment of the magnetic-wall technique eigen-equation removes the wrong cases due to the average radius approach and contains the impact of torsion of the microstrip line. Any wrong cases that are still stayed assigned to the fringing brink influences of the microstrip line which is not computed for the mathematical formularization [38].

3.4. Degenerate Modes of the Resonator

Through the study of the magnetic-wall technique, the microstripring resonator boosts two types of degenerate modes [46]. In the status of exist these modes inmicrowave cavity resonators, each of mode behaves as autonomous, this leads to occurrence the orthogonality between them. The degeneratemodes have the same resonant frequency.

The arrangement of feeders in the ring play an important role in excitation of modes. For instance, the excitation happen in one of them, unless the input and output feeders are sorted uniform. While, If these feeders are employed in non uniform case, the two modes would be seethed [46], and a littleslitting of the resonance frequency may be readilyrevealed. The twodegenerate modes can also be excited by disturbing the uniformity of the ringresonator. Wolff expanded this by a suitable perturbation patch or cut in the ring [46].

3.5. Modes of Ring Resonator

The dual mode was firstlydefined by Wolff [46]. The dual mode consists of dual splitting resonant frequenciesor degenerate modes that can beinduced by using fit perturbation patch or cut or non-symmetrical I/O feeders. The dual mode is derived basically fromsolved Maxwell's equations in the case of magnetic-wall structure of the ring resonator:

$$E_Z = [AJ_n(kr) + BN_n(kr)]\cos(n\emptyset) \tag{3.18a}$$

$$H_r = \frac{n}{j\omega\mu_\circ r}[AJ_n(kr) + BN_n(kr)]\sin(n\emptyset) \tag{3.18b}$$

$$H_\emptyset = \frac{n}{j\omega\mu_\circ}[AJ_n'(kr) + BN_n'(kr)]\cos(n\emptyset) \tag{3.18c}$$

and

$$E_Z = [AJ_n(kr) + BN_n(kr)]\sin(n\emptyset) \tag{3.19a}$$

$$H_r = \frac{n}{j\omega\mu_\circ r}[AJ_n(kr) + BN_n(kr)]\cos(n\emptyset) \tag{3.19b}$$

$$H_\emptyset = \frac{n}{j\omega\mu_\circ}[AJ_n'(kr) + BN_n'(kr)]\sin(n\emptyset) \tag{3.19c}$$

$J_n(kr)$and $N_n(kr)$represent the Bessel functions of 1st and 2nd kinds of order *n*. The wave number can be evaluated by$k = \omega\sqrt{\varepsilon_\circ\varepsilon_r\mu_\circ}$ where $\varepsilon_\circ$and $\mu_\circ$stand for free space permittivity and permeability values. The dual mode definition of the magnetic-wall model is explained in Ref. [39] as following,when a ring resonator doesn't haveexcited perturbations by symmetrical feeders, justsingle degenerate modes can be generated. The traveling counter-clockwise and clockwise on the ring resonator are perpendicular to each other in absence of coupling effect. But, in the case of perturbed means, the dual degenerate modes can be induced and coupled to each other.

From Ref.[37], the ring resonator with perturbation patch or cutresults the dual mode properly only for n odd modes. TheEq.(3.18) and Eq. (3.19) does notshow this reason instead of even mode. Moreover, the magnetic-wall model cannot statethe

dual mode of the ring resonator with complex boundary conditions. This dual mode definitioncan be describedeasily by using the transmission-line model of previous section, which explains the ring resonator as dualsimilar parallel $\lambda_g/2$ resonators [39]. While the ring resonator does not possess perturbation means and is excited by symmetrical feeders, dual similar resonators are induced and give identical frequency response, which hit each other. However, if just single $\lambda_g/2$ resonator is exited,dualvarious frequency modes are induced and couple to each other.

CHAPTER 4

DESIGN AND SIMULATION

4.1. Introduction

In this chapter, a new dual mode microstrip bandpass filter has been presented for the requirements of modern wireless communication systems. The filter has been constructed from double concentrated square loop resonators, each resonator is based on applying step impedance resonator generator on each side of closed resonator. The proposed bandpass filter has been designed using a substrate with a dielectric constant of 10.8 and thickness of 1.27mm at 2.43GHz and 5.75 GHz resonant frequencies. This filter has compact size and narrow band response which are the requirements of mobile wireless communication systems. The performance of filter has been analyzed using Microwave office software package and Sonnet simulator, which are widely adopted in microwave research and industry. The output results showed that this filter possesses very good frequency responses and high selectivity as well as blocked 2nd harmonic in out of band regions.

4.2. Adopted Step Impedance Resonator

Stepped impedance resonator (SIR) is a TEM or quasi TEM mode transmission line resonator that consists of two or more lines with different characteristic impedance. SIR is a non-uniform transmission line, which is used in the filter design either for miniaturization purposes, or shift the spurious passband to the higher frequency, or to suppress the harmonic frequencies. The SIR employed in this thesis is shown in Figure 35, it is made of two transmission line sections with two different characteristic impedances Z_1 and Z_2 with corresponding electrical lengths **x** and **y**, respectively. The input admittance that viewed from an open end can be calculated by [47] :

$$Y_{in} = \frac{2\,j\,Y_2\,(\,K\,K_1\,+\,K_2\,)(K\,-\,K_1\,K_2\,)}{K(\,1\,-\,K_1^2)(\,1\,-\,K_2^2)\,-\,2(\,1\,-\,K^2\,)K_1\,K_2}(4.1)$$

Where $K_1 = \tan(x/2)$, $K_2 = \tan(y)$ and $K = Z_2/Z_1$.
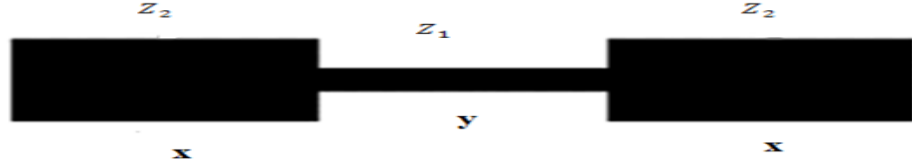

Figure 35: Schematic of the employed two-sections step impedance resonator (SIR)

4.2.1. Design and Simulation Results of Microstrip BPF

Firstly,dual concentric square loop resonators with applied SIR, has been designed at a frequency of 2.43 GHz. It has been supposed that the filter structure has been etched using a substrate with a relative dielectric constant of 10.8 and a substrate thickness of 1.27 mm. The outer resonator dimensions have been found to be 13×13 mm^2 with w= 1 mm, x =4.75 mm, y =3.5 mm and r=0.5 mm. The inner resonator has overall dimensions of 9.25× 9.25 mm^2 with w= 1 mm, x =3.25 mm ,y=2.75 mm and r=0.5 mm. The perturbation square patch side length (d) is 1 mm while the gap between I/O feeders and external resonator (g) is 0.5 mm. The procedural steps of the suggested microstrip BPF using electromagnetic modeling and simulation have been represented in the flowchart depicted in Figure 37.
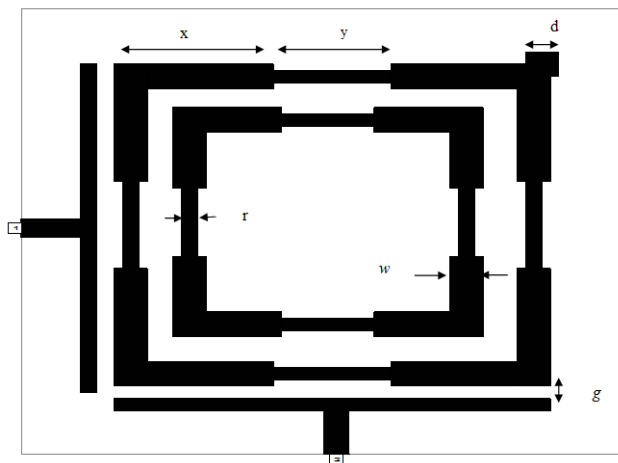

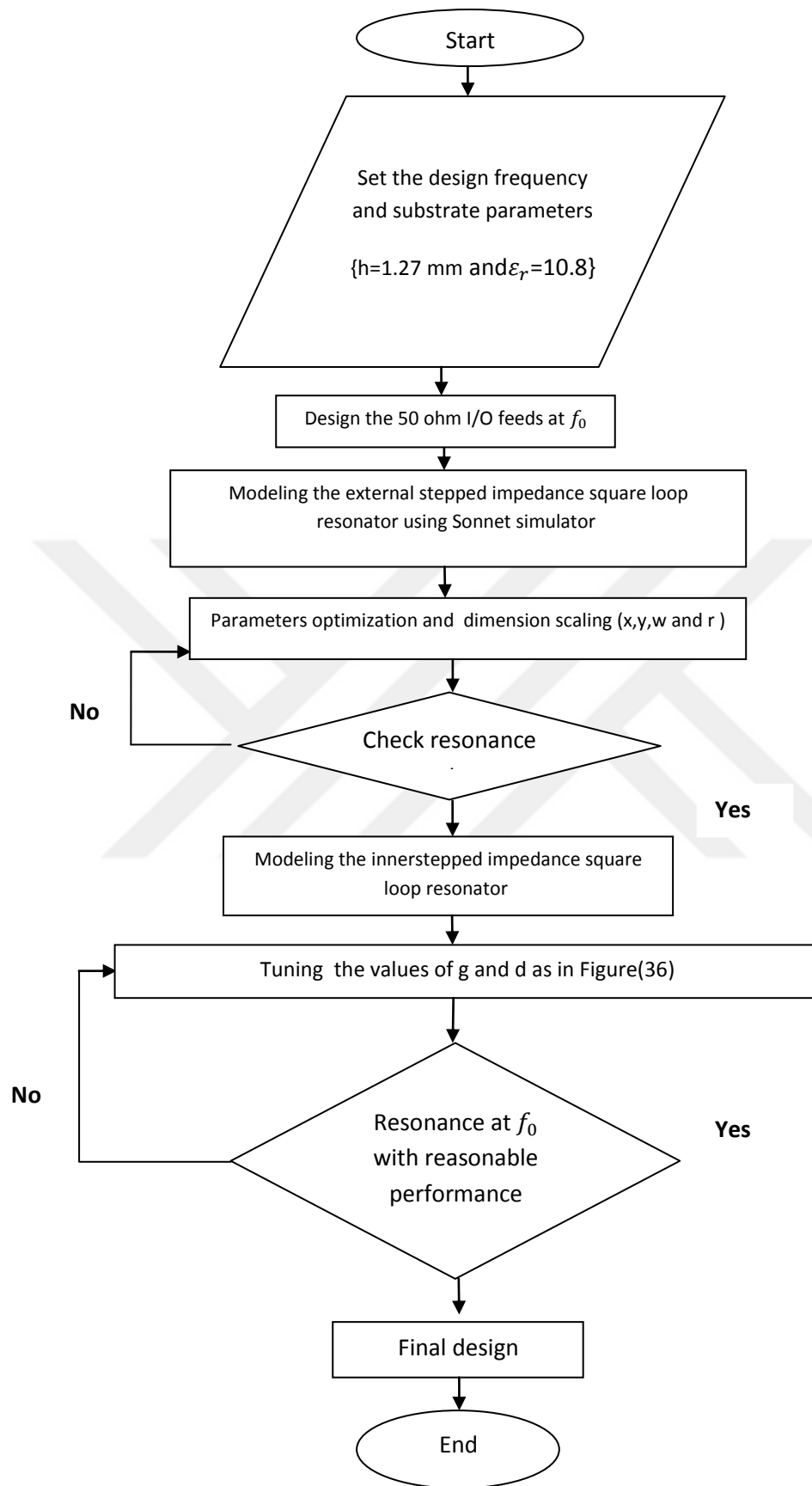Figure 36:The modeled layout of stepped impedance BPF

Figure 37:Flowchart for Moore BPF designs

;Figure 36 shows the corresponding bandpass filter design. The guided wavelength at the design frequency is calculated by (λ_g) [1-48]:

$$\lambda_g = \frac{c}{f\sqrt{\varepsilon_{eff}}} \quad (4.2)$$

$$\varepsilon_{eff} = \frac{\varepsilon_r + 1}{2} + \frac{\varepsilon_r - 1}{2} \times \frac{1}{\sqrt{1 + 12 \times \frac{h}{w}}} \quad (4.3)$$

Where ε_{eff} is effective dielectric coefficient and c is speed of light. However, ε_{eff} has been calculated as $(\varepsilon_r + 1)/2$. There are probably better approximation for this parameter, however, the additional efforts to obtain more accurate ε_{eff} is still not worth it [48].

The corresponding simulation results of return loss, S11, and transmission, S21, responses of these filters are shown in Figure 38. It is clear, that the resulting bandpass filter based on SIR application on each of concentric square loop resonator offers a quasi-elliptic transmission response with transmission zeros that are asymmetrically located around the deign frequency. Table 2 shows results of the modeled filter dimensions as designed for 2.43GHz application with corresponding filter performance parameters.

Table 2: Summary of the calculated and simulation results of the modeled filters at 2.43 GHz

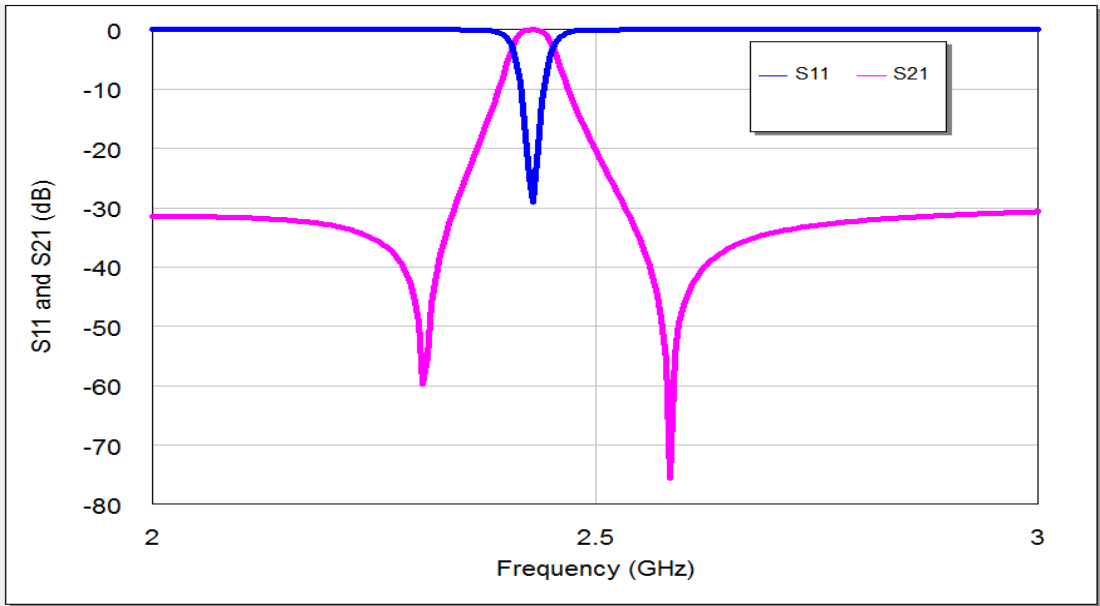| Filter Dimensions and Parameters	Magnitude
Occupied Area, mm^2	196
Band Rejection levels(dB)	-60 (left) -75 (right)
S_{11} (dB)	-29
Insertion Loss(dB)	-0.02
Bandwidth(MHz)	46

Figure 38: The return loss and transmission responses of BPF depicted in Figure36 designed for 2.43 GHz

Figure 39shows the scattering parameter simulation results of the proposed filter, where non-linear phase responses for S_{11}andS_{12} with respect to different frequencies can be observed clearly.
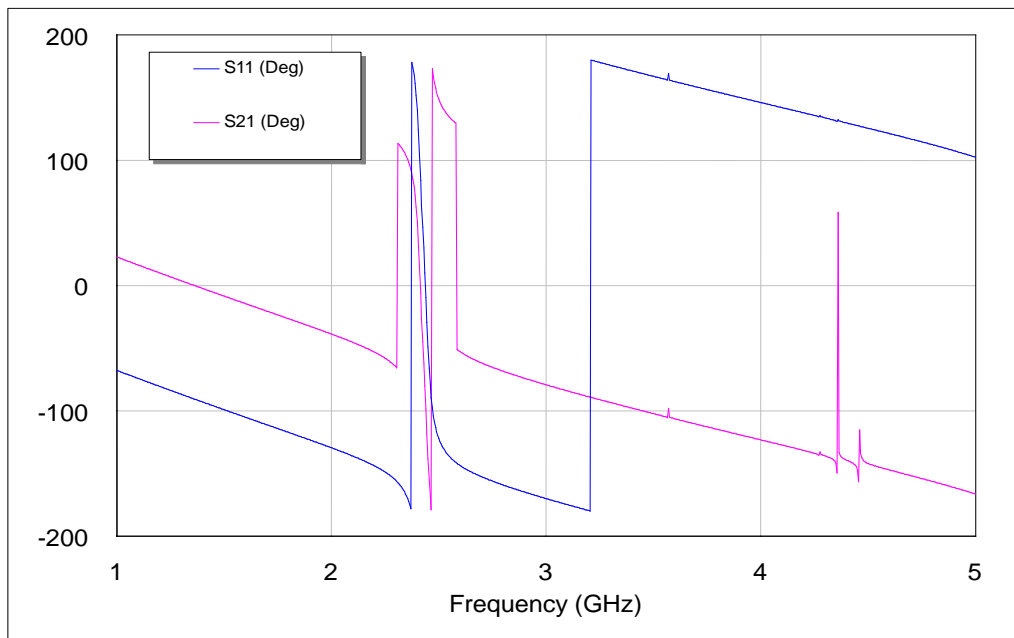

Figure 39:The phase responses of the bandpass filter depicted in Figure 36

The previous steps have been repeated, but now with a microstrip resonator designed at 5.75 GHz resonant frequency and using a substrate with the same depicted specifications. Accordingly, The outer resonator dimensions have been found to be 5.9×5.9 mm^2 with $w = 0.6$ mm, x $= 2$ mm, y $= 1.9$ mm and r$= 0.2$ mm. The inner resonator has overall dimensions of 3.9×3.9 mm^2 with $w = 0.6$ mm, x $= 1.3$ mm, y$= 1.3$ mm and r$= 0.2$ mm. The perturbation square patch side length (d) is 0.7 mm while the gap between I/O feeders and external resonator (g) is 0.2 mm. The corresponding frequency responses and phase responses are explained in Figure 40 and Figure 41 respectively. Table 3shows results of the modeled filter dimensions as designed for 5.75GHz application with corresponding filter performance parameters.
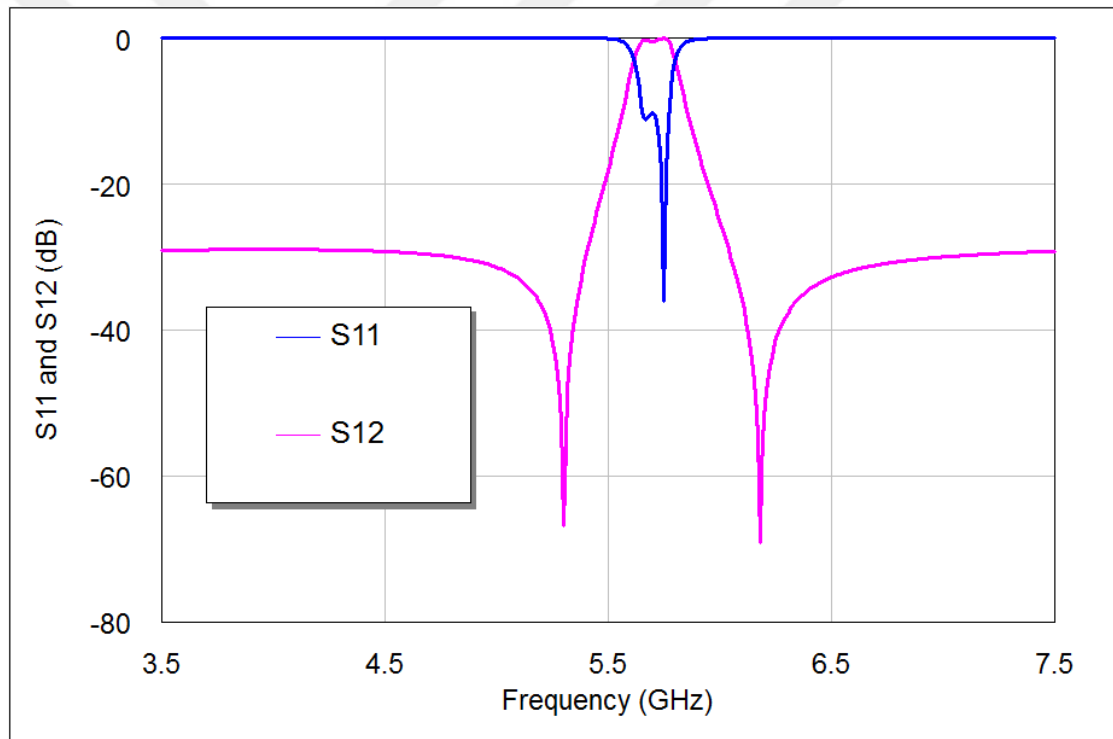

Figure 40: The return loss and transmission responses of BPF designed for 5.75 GHz

Table3: Summary of the calculated and simulation results of the modeled filters at 5.75 GHz

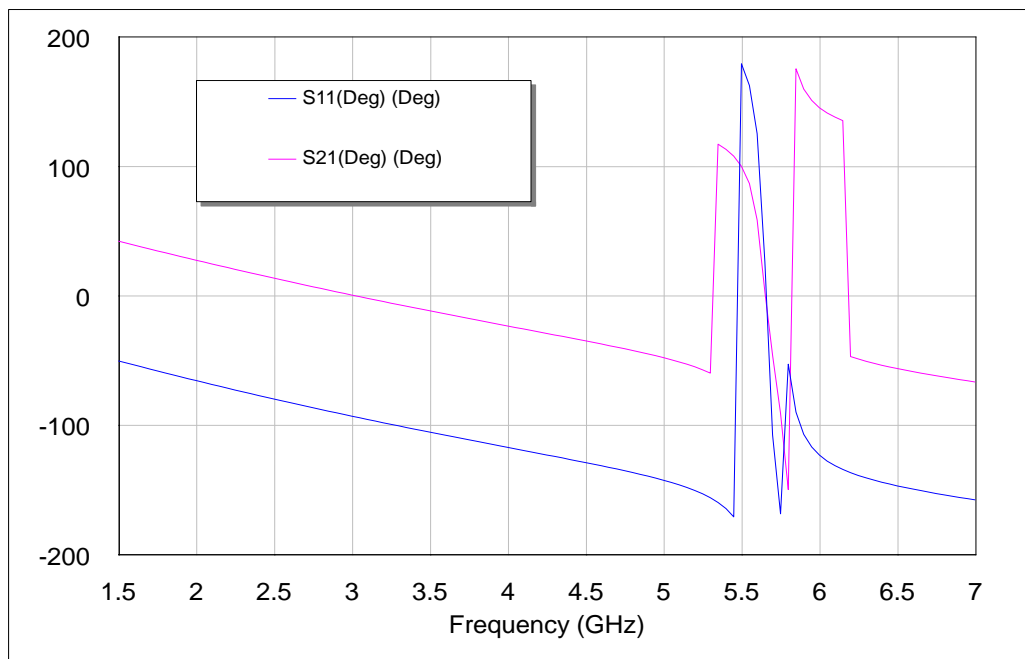| Filter Dimensions and Parameters	Magnitude
Occupied Area, mm^2	42.25
Band Rejection levels(dB)	-66 (left) -69 (right)
S$_{11}$ (dB)	-36
Insertion Loss(dB)	-0.4
Bandwidth(MHz)	183.4

Figure 41:The phase responses of the bandpass filter designed for 5.75 GHz

4.3. Discussion of the Results

Filter structures, as in Figure 36, has been modeled and analyzed at operating frequencies 2.43GHz and 5.75 GHz using Microwave Office 2009 electromagnetic simulator from Advanced Wave Research (AWR) Inc. The output frequency responses of these filters are shown in Figure38 and Figure 40, respectively. The frequency responses of these filters have low insertion loss and good return loss as well as narrow band at -3dB regions which are very good features in the basics of filter theory. Tables2 and 3, demonstrated the simulated dimensions of the proposed

microstrip filters. All structures have been modeled at the design frequency and using the same substrate material.

Figure 39 and Figure 41show the non-linear phase response for S11 and S12 with respect to different frequencies .The S11 and S21 phase responses are intersected to each other in the regions nearby design frequency   .

Frequency harmonics is often accompanying the bandpass filter responses which is consequently reduces the performance of these filters.Harmonic frequency represents an integermultiple of the fundamental frequency, i.e. if the fundamental frequency is f, the harmonics have frequencies $2f$, $3f$, $4f$, . . . etc.

Due to the effects of applied SIR in proposed filters, Figure 42 and Figure43, show the out-of-band transmission responses of the two filters designed for 2.43GHz and 5.75 GHz respectively. It is very obvious that the responses of modeled filters indicate blocked 2nd harmonic in out of regions.This property is very requested in high reliability wireless communication systems.
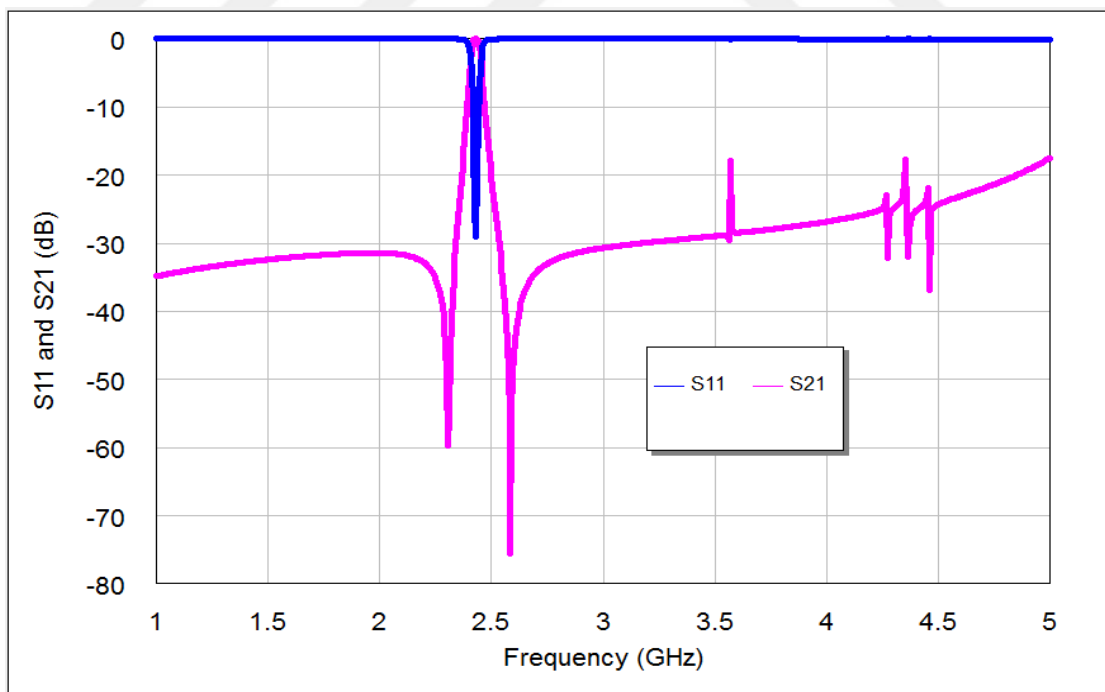

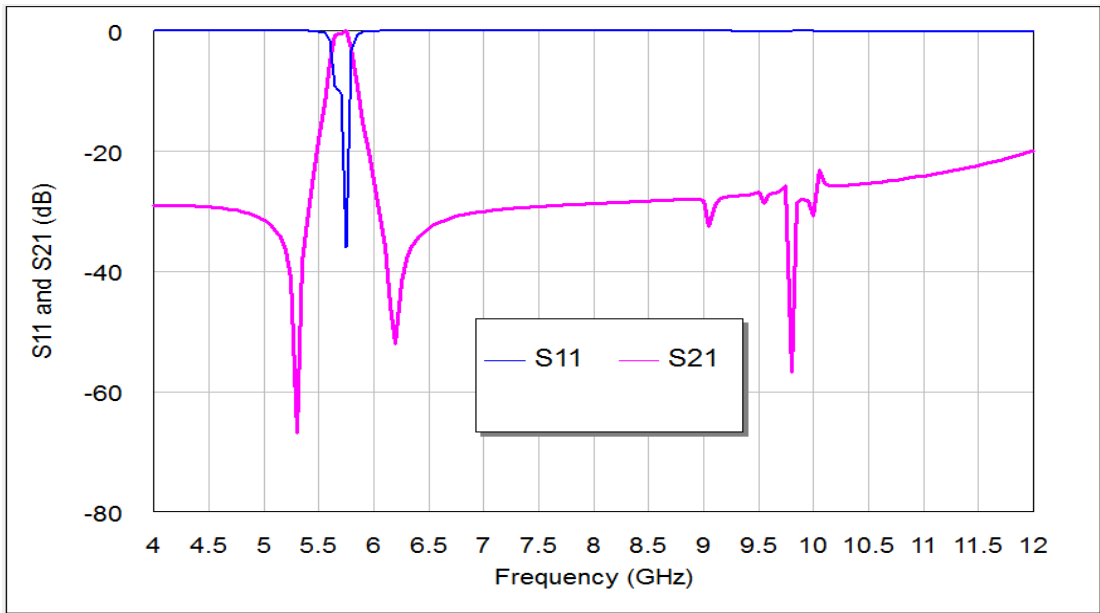Figure 42:The out-of-band transmission responses of the proposed filter designed for 2.43 GHz fundamental frequency

Figure 43:The out-of-band transmission responses of the proposed filter designed for 5.75 GHz fundamental frequency

Figure 44 andFigure 45, respectively demonstrate surface current density simulation results using Sonnet simulator at 2.43GHz and 5.75 GHz fundamental frequencies while Figure 46 andFigure 47,show surface current density distributions at 3.3GHz and 6.5 GHz in stopband regions. In these figures, the red color indicates the maximum coupling effect while the blue color indicates the minimum one.The maximum surface current densities can be seen at the design frequency, which is straightforward from the fact that low losses are present and the desired resonant frequency is within higher excitation condition. On the contrary, the lowest current densities can be noticed at 3.3GHz and 6.5 GHz in stopband region. In this case, weakest coupling can be seen, which is given by the fact that the designed filter are not being excited and, therefore, provide a strong rejection in an otherwise passband structure. Consequently, the proposed techniques can be generalized as a flexible design tool for compact microstrip bandpass filters for a wide variety of wireless communication systems. Also, the proposed filter designs can be applied to many other wireless communication systems, in this case, the filter dimensions must be scaled up or down depending on the required operating frequencies.
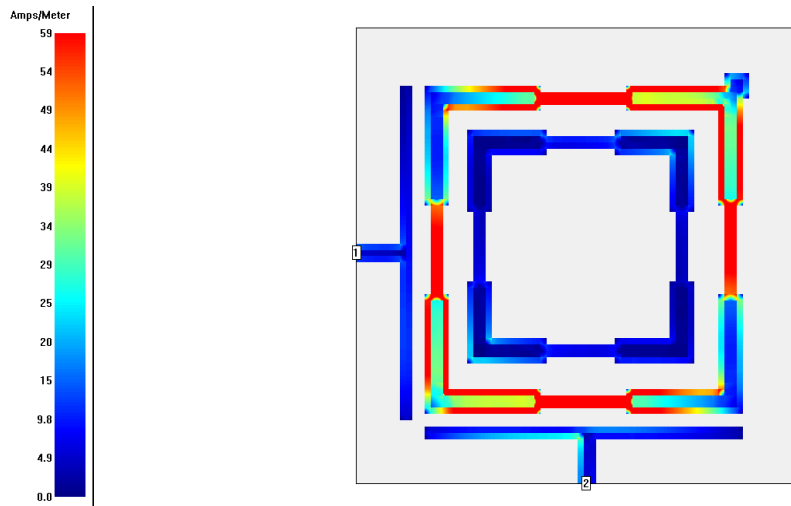
Figure 44:Simulated current density distributions of the proposed BPF at 2.43 GHz fundamental frequency (in passband region)
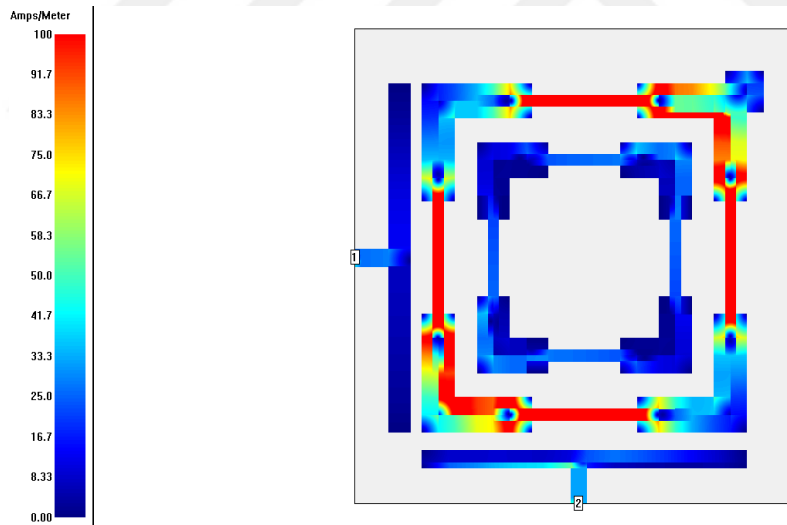

Figure 45:Simulated current density distributions of the proposed BPF at 5.75 GHz fundamental frequency (in passband region)
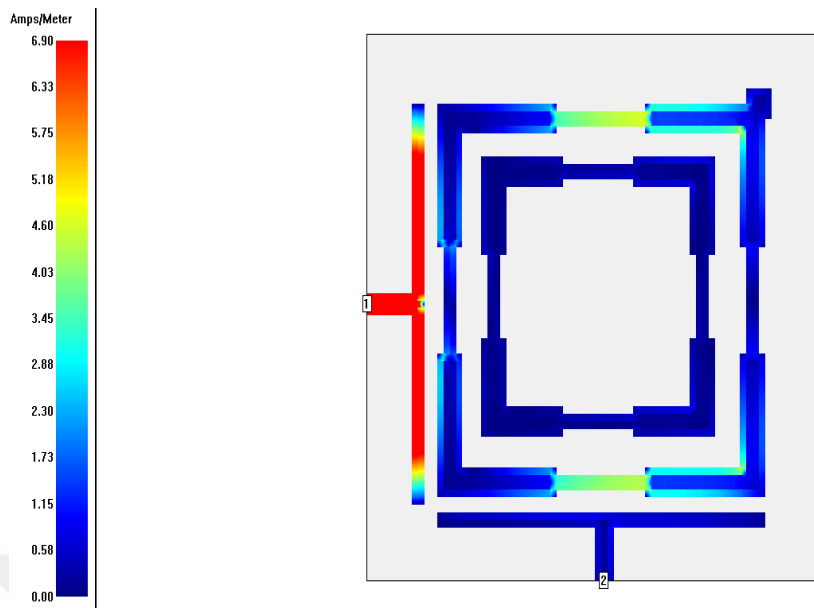
Figure 46:Simulated current density distributions of the proposed BPF at 3.3 GHz (in stopband region)
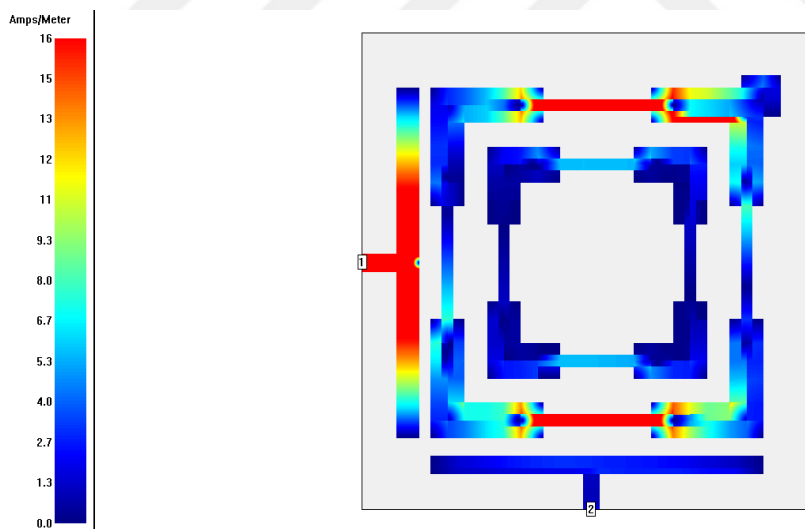
Figure 47:Simulated current density distributions of the proposed BPF at 6.5 GHz (in stopband region)

Generally in degenerate dual-mode case, the bandpass filter response can be obtained through the excitation of the two degenerate modes by input output feed lines and adjusting the coupling between the two modes by adding suitable form of perturbation within the resonators. In this thesis, small square patch that acts as perturbation effect is applied to proposed filter design, atlocations that are

assumed at an angle 45^0 offset from its two orthogonal modes. This perturbation can be in the form of a small square patch with a side length d, added to the upper right corner of the conventional square patch as shown in Figure 36. For 5.75 GHz design case, we see from Figure48, that increasing d, the side length of small perturbation square patch at the right top corner, causes S21first to move rapidly upward toward the ideal 0dB point and then split into two visible peaks. Ideally there would be no coupling between the two modes at d = 0 mm.It is seen from these figures that the splitting of frequency between the two modes and the coupling effect are increased as the perturbation size d, is increased.
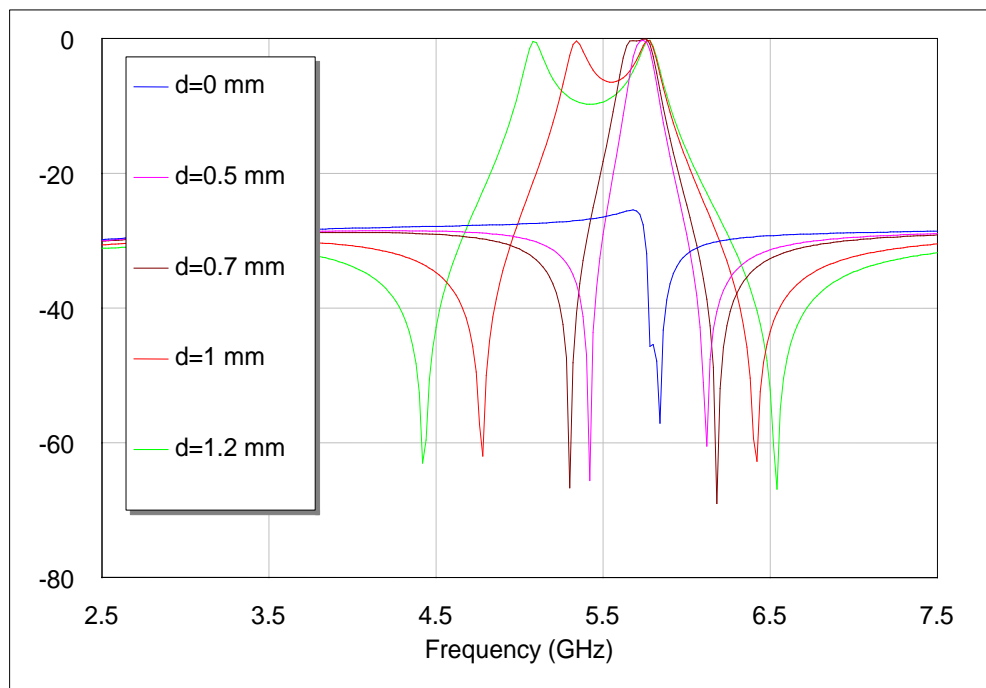
Figure 48:Simulated transmission responses, S21, of proposed BPF as a function of d in units of mm.

The external quality factor Q_{ext} decreases as d parameter increases while the coupling coefficient K_{12} increases with increasing the perturbation size d, while as can be observed from Figure 49 and Figure 50 respectively .
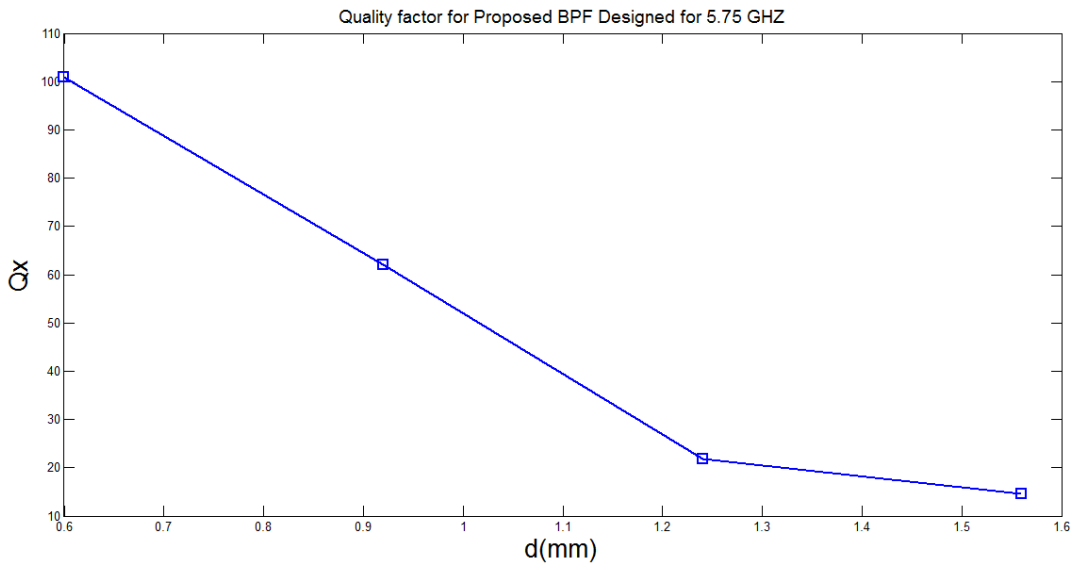
Figure 49: External quality factor Q_{ex} as function of d
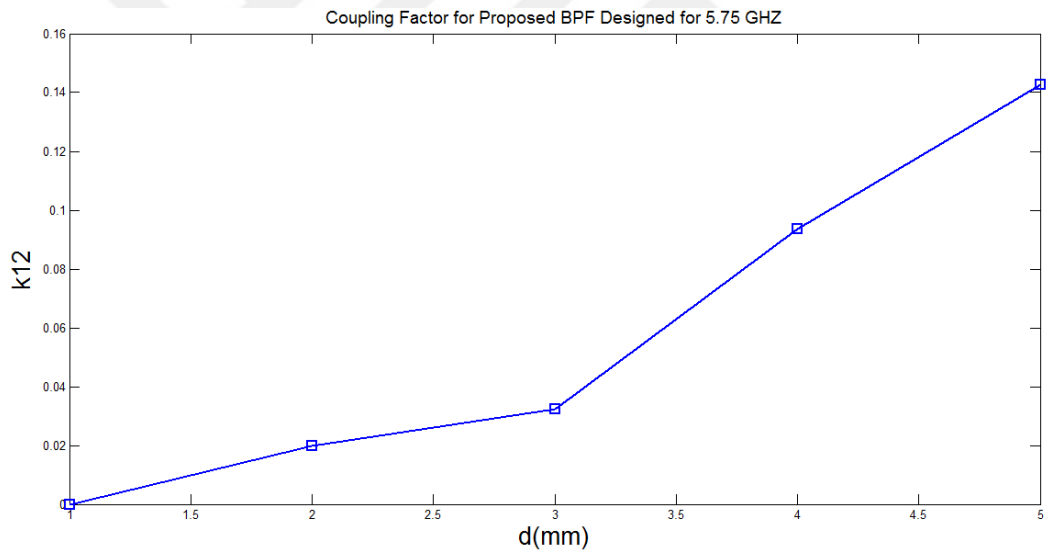
Figure 50: Coupling coefficient K_{12} as function of d

CHAPTER 5

CONCLUSIONS AND SUGGESTIONS FOR FUTURE WORKS

5.1. Conclusions

New narrow band microstrip bandpass filter designs by applying SIR generator on each side of square loop resonator have been introduced in this dissertation for first time. The proposed filter structures have been composed of dual concentric microstrip resonators with a dielectric constant of 10.8 and thickness of 1.27mm at 2.43GHz and 5.75 GHz center frequencies. The new filter designs have small sizes and good transmission and return loss characteristics with blocked higher harmonics in out of band regions, which are very interesting features required for modern wireless applications.

A perturbation size was changed for many values, for proposed microstrip bandpass filters that have been investigated, to see the effect of the perturbation size on the performance of filters. As observe here

 a. The coupling coefficient K_{21} is increased as the perturbation size increased.

 b. The splitting of frequency between the two modes is increased as the perturbation size increased.

 c. The loaded quality factor Q_{ex} is decreased as the perturbation size increased.

5.2. Suggestions for Future Works

The field of producing miniaturized bandpass filters for different wireless communication systems, using different concepts is still growing and much can be done in this field.

Some of the suggestion that can be recommended in this issue can be summarized as a follows:

1. Relating the work presented in this thesis, additional investigations can be performed to achieve the experimental measurements for modeled designs.
2. Make use of the compact filters satisfied in this work to design a narrower response filters with 4 poles and more. These types filter with narrower and sharper responses are needed in many wireless systems working with adjacent bands.

Applying SIR generator on triangular ring resonators with open or closed loop to get filters with more compact small size and better performances.

REFERENCES

1. **HongJ. S. and Lancaster M.J., (2001),***"Microstrip Filters for RF/MicrowaveApplications"*,JohnWiley&Sons, pp.315-360.

2. **Zverev A. I., (1967),***"Handbook of Filter Synthesis"*, New York, John Wiley & Sons, pp. 396-421.

3. **Hong J. S. and Lancaster M. J., (1996),***"Compact Microwave Elliptic Function Filter Using Novel Microstrip Meander Open-Loop Resonators"*, Electronics Letters, vol. 32, no. 6, pp. 563–564.

4. **Craven G. F. and Mok C. K., (1971)**, *"The Design of Evanescent Mode Waveguide Bandpass Filter for A Prescribed Insertion Loss Characteristic"*, IEEE Trans. Microwave Theory Techniques, vol. 19, no. 3, pp. 295–308.

5. **Hong J. S. and Lancaster M. J., (1995)**, *"Microstrip Bandpass Filter Using Degenerate Modes of A Novel Meander Loop Resonator"* , IEEE Microwave and Guided Wave Letters, vol. 5, no. 11, pp. 371-372.

6. **Hong J. S. and Lancaster M. J., (2000),***"Design of Highly Selective Microstrip Bandpass Filters with A Single Pair of Attenuation Poles at Finite Frequencies"*, IEEE Transactions on Microwave Theory and Techniques, vol. 48, no. 7,pp. 1098-1107.

7. **Matsuo M.,Yabuki H. and Makimoto M., (2001),***"Dual-Mode Stepped-Impedance Ring Resonator for Bandpass Filter Applications"*, IEEE Transactions on Microwave Theory and Techniques, vol. 49, no. 7,pp. 1235-1240.

8. **Görür A., (2002),** *"A Novel Dual-Mode Bandpass Filter with Wide Stopband Using The Properties of Microstrip Open-Loop Resonator"*, IEEE Microwave and Wireless Component Letters, vol. 12, pp. 386-388.

9. **Görür A., Karpuz C. and Akpinar M., (2003),** *"A Reduced-Size Dual-Mode Bandpass Filter with Capacitively Loaded Open-Loop Arms"*, IEEE Microwave and Wireless Component Letters, vol. 13, no. 9, pp. 385-387.

10. **Lugo C.and Papapolymerou J., (2005),** *"Bandpass Filter Design Using A Microstrip Triangular Loop Resonator with Dual-Mode Operation"*, IEEE Microwave and Wireless Component Letters, vol. 15, no. 7, pp. 475-477

11. **Wang Y.X.,Wang B. Z. and Wang J., (2007),** *"A Compact Squre Loop Dual-Mode Bandpass Filter with Wide Stop-Band"*,PIER, Progress in Electromagnetic Research, vol. 77, pp. 67–73.

12. **Hashemi S.K.and Syahkal D.M., (2009),** *"A New Generation of Microwave Bandpass Filters Using Multilayer Ring Resonators"*, IEEE.,pp. 1341-1344.

13. **Zhou M.,Tang X. and Xiao F., (2010),** *"Miniature Microstrip Bandpass Filter Using Resonator-Embedded Dual-Mode ResonatorBased on Source-Load Coupling"*, IEEE Microwave and Wireless Component Letters, vol. 20, no. 3, pp.139-141.

14. **Phromloungsria R.,Thammawongsaa N.and Arunvipasb P., (2011),** *"Design of Compact Microstrip Stepped-impedance Resonator Bandpass Filters"*, Science Direct, Procedia Engineering, vol. 8, pp. 30–35.

15. **Bukuru D.,Song K.,Ren X. and Zhao M., (2014),** *"Miniaturized Microstrip Bandpass Filter Designed Using Rectangular Dual Spiral Resonator"*, Published by Elsevier GmbH International Journal of Electronics and Communications,AEUE-51160, pp. 1- 4.

16. **Davis W. A. andAgarwal K., (2001),**_"Radio Frequency Circuit Design"_, John Wiley & Sons, Inc, New York, pp. 166–173.

17. **Pozar D. M., (2005),**_"Microwave Engineering"_, John Wiley & Sons, New York, pp. 130–235.

18. http://www.mwrf.com/Articles/ArticleID/19725/19725.html, (Data Download Date: 15.01.2014).

19. http://www.pcbprototype.net/article/Design Techniques4.html,(Data Download Date: 05.02.2014) .

20. **Edwards T. C. andSteer M. B., (2000),**_"Foundations of Interconnect and Microstrip Design"_, John Wiley & Sons, New York, pp.87-158.

21. http://www.mwrf.com/Articles/ArticleID/20743/20743.html,(Data Download Date: 16.02.2014).

22. http://www.microwaves101.com/encyclopedia/propagation.cfm,(Data Download Date: 25.02.2014).

23. **Fooks E. H. andZakarevicius R. A., (1990),**_"Microwave Engineering Using Microstrip Circuits"_, Prentice Hall, New York, pp.77-105.

24. **Russer P., (2003),**_"Electromagnetic, Microwave Circuit and Antenna Design for Communications Engineering",_ Artech House Publishers, New York, pp. 233–247.

25. **Martin A. P., (1978),** _"Applied Electromagnetics"_, McGraw-Hill Book Company, New York, pp. 203-236.

26. **Nibler F., (1996),** _"High Frequency Circuit Engineering"_, IEEE Circuit and Systems Series 6, UK, pp.115-156.

27. http://www.microwaves101.com/encyclopedia/sparameters.cfm, (Data Download Date: 01.03.2014).

28. **Edwards T., (1992),** *"Foundations for Microstrip Circuit Design"*, John Wiley & Sons, West Sussex, pp.245-284.

29. **Ruymbeke G. V., (1995),** *"Filtres Continus Integres Programmables"*, Ph.D. Thesis, EPFL, Lausanne, pp.44-52.

30. **Ruymbeke G., Enz C. C.,Krummenacher F. and Declercq M., (1997),** *"A BiCMOS Programmable Continuous-Time Filter Using Image-Parameter Method Synthesis and Voltage-Companding"*, IEEE Journal of Solid-State Circuits, pp.377-387.

31. **Kuo F. F., (1966),** *"Network Analysis and Synthesis"*, John Wiley & Sons, New York, pp. 212-247.

32. **Temes G.C. andLapatra J.W., (1977),** *"Introduction to Circuit Synthesis and Design"*, McGraw-Hill, New York, pp. 144-167.

33. **Matthaei G.L.,Young L. and Jones E. M., (1964),** *"Microwave Filters, Impedance-Matching Networks, and Coupling Structures"*, McGraw-Hill, New York, pp. 209-250.

34. **Coh S. B., (1958),** *"Parallel-Coupled Transmission-Line-Resonator Filters"*, IRE Trans. Microwave Theory and Techniques, pp.75-90.

35. **WolffI.and Knoppik N., (1971),** *"Microstrip Resonator and Dispersion Measurements Microstrip Lines"*, Electronics Letters, vol. 7, pp. 779-781 .

36. **Wu Y. and Rosenbaum F. J., (1973),** *"Mode Chart for Microstrip Resonators"*, IEEE Trans. Microwave Theory Technology, vol. 21, pp. 487-489.

37. **Chang K.,Martin T. S., Wang F. and Klein J. L., (1987),** *"On The Study of Microstrip Ring and Varactor-Tuned Circuits"*, IEEE Trans. Microwave Theory Technology, vol. 35, pp. 1288-1295.

38. **Hsieh L. and Chang K., (2003),***"Simple Analysis of The Frequency Modes for Microstrip Ring Resonators of Any General Shape and The Correction of An Error in Literature",* Microwave and Optical Technology Letters, vol. 38, pp. 209-213.

39. **Hsieh L. and Chang K., (2002),***"Equivalent Lumped Elements G, L, C and Unloaded Qs of Closed- and Open-Loop Ring Resonators"*, IEEE Trans. Microwave Theory Technology, vol. 50, pp. 453-460.

40. **Pintzos S. G. and Pregla R., (1978),***"A Simple Method for Computing The Resonant Frequencies of Microstrip Ring Resonators"*, IEEE Trans. Microwave Theory Technology, vol. MTT-26, pp. 809–813 .

41. **Wolff I. and Tripathi V. K., (1984),***"The Microstrip Open-Ring Resonator"*, IEEE Trans. Microwave Theory Technology, vol. MTT-32, pp.102–106 .

42. **Gopalakrishnan G. K. and Chang K., (1990),***"Bandpass Characteristics of Split-Modes in Asymmetric Ring Resonators"*, Electronics Letters, vol. 26, pp. 774-775.

43. **Hong J. S. and Lancaster M. J., (1995),***"Microstrip Bandpass Filter Using Degenerate Modes of A Novel Meander Loop Resonator"*, IEEE Microwave Guided Wave Letters, vol. 5, pp. 371-372.

44. **Yu W. and Chang K., (1997),***"Transmission-Line Analysis of A Capacitively Coupled Microstrip-Ring Resonator"*, IEEE Trans. Microwave Theory Technology, vol. 45, pp. 2018-2024.

45. **Chang K., (1996),***"Microwave Ring Circuits and Antennas"*, Wiley , New York, pp. 102-106.

46. **Wolff I., (1972),** *"Microstrip Bandpass Filter Using Degenerate Modes of Microstrip Ring Resonator"*, Electronics Letters, vol.12, pp. 302-303.

47. **Mokhtaari M., Jens B. and Amari S., (2006),** *"New Reduced-Size Step-Impedance Dual-Band Filters withEnhanced Bandwidth and Stopband Performance"*, IEEE MTT-S Int. Microwave Symp. Dig., pp.1181-1184.

48. **Waterhouse R. B.,(2003),** *"Microstrip Patch Antennas: A Designer'sGuide",*Kluwer Academic Publishers, pp.45-77.

CURRICULUM VITAE

PERSONAL INFORMATION

Surname, Name: AL-MIHRAB, Mohammed Abdulrazzaq Azeez

Nationality: Iraqi (IQ)

Date and Place of Birth: 15January 1988 , Talafar, Mosul

Marital Status: Married

Phone: +9647706128628

Email:1988moh2014@gmail.com

EDUCATION

Degree	Institution	Year of Graduation
M.Sc.	Çankaya University Electronic and Communication Engineering	2014
B.Sc.	Mustansiriya University Electrical Engineering	2011
High School	AL Fager for boys	2006

FOREIGN LANGUAGES

Advanced English and Turkish

HOBBIES

Reading of social books, Learning languages, Swimming.